2023

Labile carbon and soil texture control nitrogen transformation in deep vadose zone

Lidong Li

Jordan Shields

Daniel D. Snow

Michael Kaiser

Arindam Malakar

Labile carbon and soil texture control nitrogen transformation in deep vadose zone

Lidong Li,[1] Jordan Shields,[2] Daniel D. Snow,[2] Michael Kaiser,[1] & Arindam Malakar[2]

1 University of Nebraska-Lincoln, Department of Agronomy and Horticulture, 1875 N 38th St, 279 Plant Sciences Hall, PO Box 830915, Lincoln, NE 68583-0915, USA

2 School of Natural Resources and Nebraska Water Center, Part of the Robert B. Daugherty Water for Food Global Institute, University of Nebraska, Lincoln, NE, 68583-0844, USA

Corresponding author — A. Malakar, email: amalakar2@unl.edu

Highlights

- 21.7–1043.6 gm−2 of inorganic N (nitrate and ammonium) was stored in vadose zone.
- Thicker vadose zone sediments stored more inorganic N.
- N transformation in deep vadose can occur with the presence of organic C.
- Mineralization and nitrification occurred at the 19 m depth with sandy soil texture.
- Denitrification occurred at the 12 m soil depth with clay soil texture.

Published in *Science of the Total Environment* 878 (2023) 163075
doi:10.1016/j.scitotenv.2023.163075

Submitted 27 January 2023; revised 10 March 2023; accepted 22 March 2023; published 25 March 2023

Abstract
Understanding transient nitrogen (N) storage and transformation in the deep vadose zone is critical for controlling groundwater contamination by nitrate. The occurrence of organic and inorganic forms of carbon (C) and nitrogen and their importance in the deep vadose zone is not well characterized due to difficulty in sampling and the limited number of studies. We sampled and characterized these pools beneath 27 croplands with different vadose zone thicknesses (6–45 m).We measured nitrate and ammonium in different depths for the 27 sites to evaluate inorganic N storage. We measured total Kjeldahl nitrogen (TKN), hot-water extractable organic carbon (EOC), soil organic carbon (SOC), and $\delta^{13}C$ for two sites to understand the potential role of organic N and C pools in N transformations. Inorganic N stocks in the vadose zone were 21.7–1043.6 gm^{-2} across 27 sites; the thicker vadose zone significantly stored more inorganic N ($p < 0.05$). We observed significant reservoirs of TKN and SOC at depths, likely representing paleosols that may provide organic C and N to subsurface microbes. The occurrence of deep C and N needs to be addressed in future research on terrestrial C and N storage potential. The increase of ammonium and EOC and $\delta^{13}C$ value in the proximity of these horizons is consistent with N mineralization. An increase of nitrate, concurrent with the sandy soil texture and the water-filled pore space (WFPS) of 78%, suggests that deep vadose zone nitrification may be supported in vadose zones with organic-rich layers such as paleosol. A profile showing the decrease of nitrate concentrations, concurrent with the clay soil texture and the WFPS of 91%, also suggests denitrification may be an important process. Our study shows that microbial N transformation may be possible even in deep vadose zone with co-occurrence of C and N sources and controlled by labile C availability and soil texture.

Keywords: Vadose zone, Nitrate, Ammonium, Total Kjeldahl nitrogen, Hot-water extractable organic carbon, Soil organic carbon, $\delta^{13}C$ value

1. Introduction

Nitrogen (N) fertilizer application in agricultural ecosystems leads to a surplus of soil N and N leaching, primarily as nitrate, to groundwater. It has been estimated that as much as 29 % of surface N input is leached, mainly in the form of nitrate, into deep soil below 3 m and to groundwater beneath intensively-farm cropland (Weitzman et al., 2022). Irrigated, intensively-farmed cropland on sandy soils is especially vulnerable to nitrate leaching (Burow et al., 2010; Exner et al., 2014). Since the deep vadose zone can be a substantial reservoir of nitrate (Ascott et al., 2017), nitrate contamination in groundwater is significantly controlled by the thickness of the vadose zone (Voisin et al., 2018). Long travel times in thicker vadose zone may delay or reduce the nitrate contamination in groundwater resulting from excess fertilizer application (Ascott et al., 2017; Juntakut et al., 2019; Weitzman et al., 2022).

In comparison to nitrate, labile carbon, e.g., dissolved organic carbon (DOC) or water-extractable organic carbon (EOC), can be more efficiently retained in the vadose zone regardless of its thickness (Voisin et al., 2018). Soil organic carbon (SOC) is one of the most important influencing factors for N transformation by mediating microbial activity and community (Wu et al., 2021). Soil texture is another critical factor for controlling N transformation by affecting rates of nitrification, denitrification, and dissimilatory nitrate reduction to ammonium (DNRA) as it can control soil water filled pore space and, thus, aerobic conditions (Mekala and Nambi, 2017; Pihlatie et al., 2004). With most studies focusing mainly on the topsoil, very few studies have evaluated the potential occurrence of N transformations that may support denitrification and anaerobic ammonium oxidation (anammox) in deep vadose zone sediments (Jia et al., 2018; Zhu et al., 2018). One study has reported the likelihood of anammox, nitrification, and denitrification in unconfined aquifer soils in the vadose zone (Wang et al., 2017). The occurrence and importance of microbial N transformations, (e.g., mineralization, nitrification, denitrification, DNRA, and anammox) in the deep vadose zone is debatable and has not been well characterized (Weitzman et al., 2022; Xin et al., 2019).More complete information is needed for evaluating the potential for microbial N transformation and predicting risks of groundwater contamination from excess N fertilizer application beneath irrigated cropland. This paper aims to report on the co-occurrence of inorganic and organic C and N, to better understand how transient N storage and transformation may occur in the deep vadose zone. We measured ammonium and nitrate stocks in the vadose zone to evaluate the effect of vadose zone thickness on N storage. We measured EOC, SOC, and $\delta^{13}C$ value to examine the potential effect of C availability on N transformation.

2. Material and methods

Vadose zone sediments were collected in the Central Platte Natural Resources District (CPNRD) in central Nebraska (Fig. S1). Much of the surface soil is a Hastings silt loam with a 1–3 % slope and high sand content (Fig. S2). The CPNRD identified the sampling locations to evaluate the effects of land use and irrigation practices on nitrate concentrations in local groundwater starting in the 1990s. Vadose zone sediments were sampled from 27 sites between 2016 and 2019. See the coordinates and sampling dates in Table S1. These sites were primarily on irrigated croplands with corn or corn/soybean rotation with manure or inorganic N fertilizer application (Table S2). Deep cores were collected using a Central Mine and Equipment drill rig outfitted with a hollow stem auger and split spoon core barrel containing

acrylic liners, or a Geoprobe direct-push sampling rig (Fig. S3). Continuous cores were collected wherever possible from the root zone to the regional water table. Core lengths ranged from 6 m to 45 m depending on the depth of the water table. Some coring locations had samples that penetrated the saturated zone, presumably due to an indistinct water table (Table S3). Cores were extruded, air-dried, and composited in 70 cm sections or less depending on changes in lithology. Nitrate- and ammonium-N was extracted and measured in composites from all 27 sites, while two were selected for measurement of total Kjeldahl nitrogen (TKN), hot-water extractable organic carbon (EOC), soil organic carbon (SOC), and soil $\delta^{13}C$ value. TKN, a measure of both ammonia-N and organic N, was used to quantify soil organic nitrogen (SON). Soils were acid-fumigated to remove carbonate before SOC and $\delta^{13}C$ measurement to remove inorganic C. Sediment texture was described using a Soil Texture Pyramid according to particle size analyses (Kettler et al., 2001). Vadose zone thickness was divided and categorized as lower (6–23 m) and higher thickness (24–45 m) for statistical analyses (Table S4). The 23 m thickness was chosen as an arbitrary depth because it is half the highest vadose thickness of 45 m sampled in this study. A one-way mixed model ANOVA was conducted to test the effect of vadose zone thickness on stocks of nitrate-N and ammonium-N, which included all 27 sites (Glimmix procedure; SAS 9.4, SAS Institute Inc., Cary, NC, USA). Vadose zone thickness was the fixed factor, and the individual site was the random factor. Least Squares Means were compared by Fisher's Least Significant Difference. Data were log-transformed to achieve normal distribution. The univariate procedure was used to check the normality of residuals. The Shapiro-Wilks test determined normality. Equal variance was determined by Levene's test. Significance was set at the 0.05 level. Results were reported as untransformed mean ± standard error.

3. Results and discussion

Inorganic N (nitrate-N and ammonium-N) stocks in the vadose zone ranged from 21.7 to 1043.6 g m^{-2} across 27 sites, with large variations due to vadose zone thickness (6–45 m) and N application history (Tables S4 and S2). Vadose zone N storage can serve as a buffer for slowing nitrate leaching into groundwater (Weitzman et al., 2022). Higher thickness vadose zone (24–45 m) in the present study was found to contain more inorganic N than the lower thickness vadose zone (6–23 m, $p < 0.05$, Fig. 1A). The average storage capacity of inorganic N in each cubic meter of the vadose zone did not significantly change with the thickness ($p > 0.05$, Fig. 1B). In our 27 sites, ammonium-N concentrations were largely consistent throughout different soil

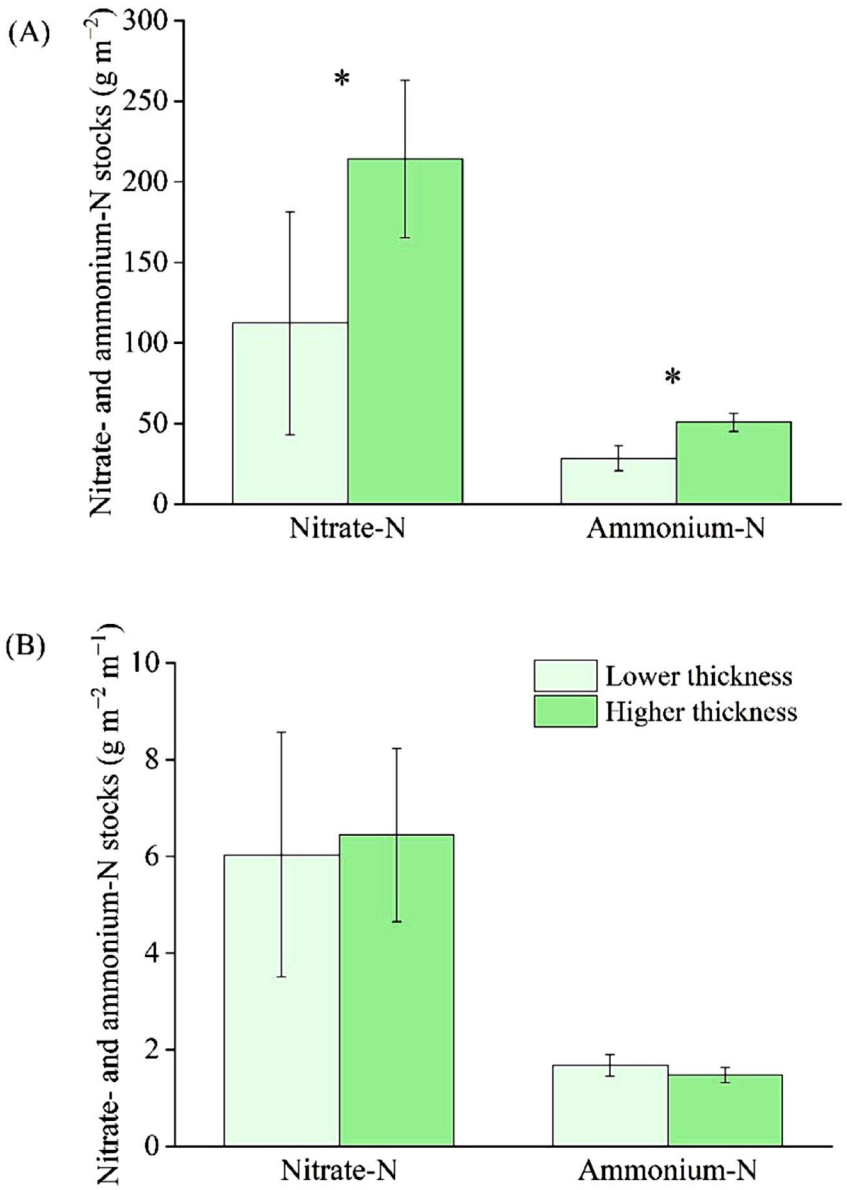

Fig. 1. Stocks of nitrate-nitrogen (N) and ammonium-N in vadose zones of different thicknesses. Lower thickness vadose zone, 6–23 m (n=9); higher thickness vadose zone, 24–45 m (n=18). Stars indicate significant differences between lower and higher thickness at the 0.05 confidence level. Black bars represent standard errors. **(A)** Nitrate-N and ammonium-N stocks in the entire vadose zone; **(B)** nitrate-N and ammonium-N stocks in the entire vadose zone divided by the vadose zone thickness. See Table S4 for stocks in individual sites.

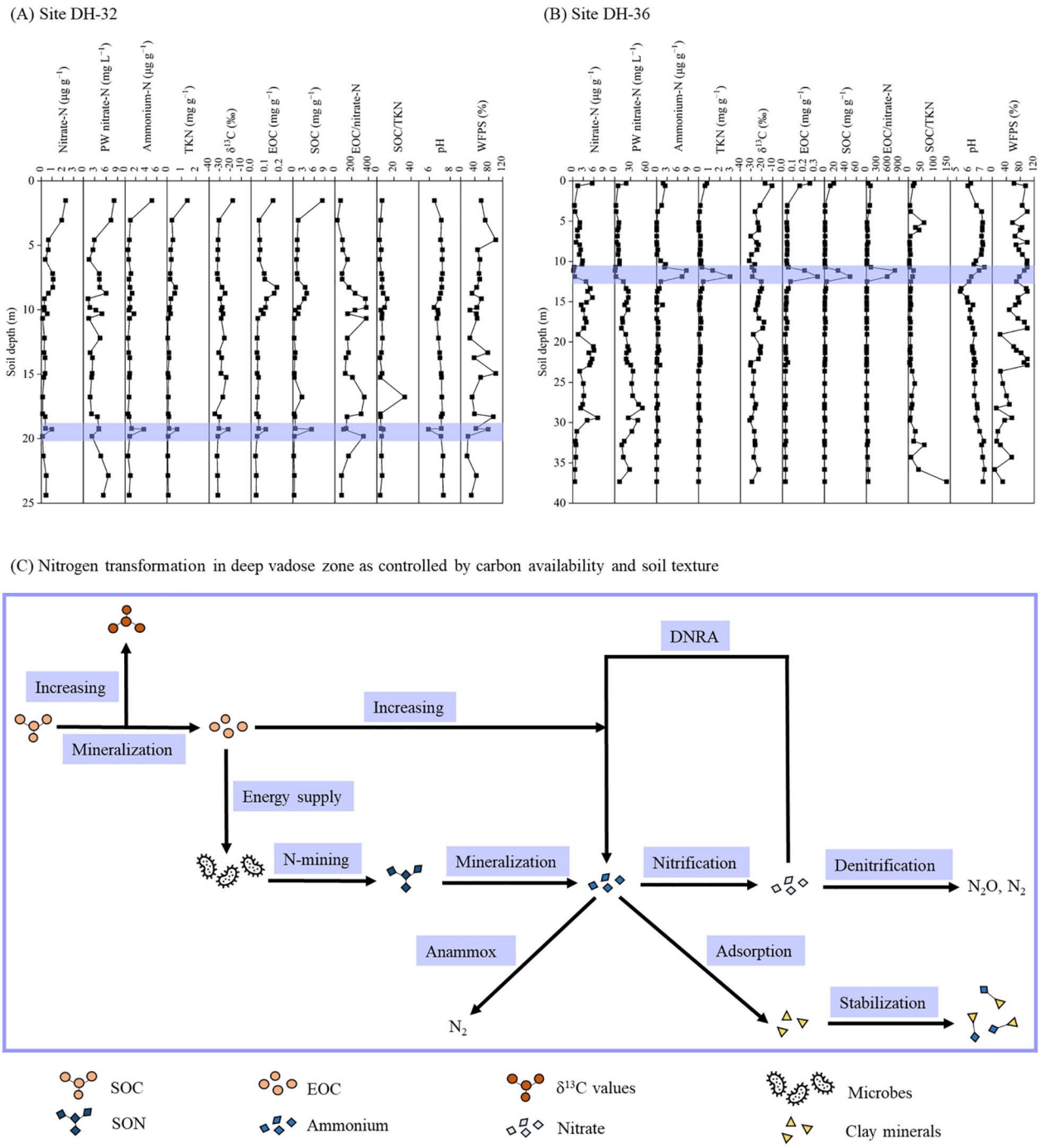

Fig. 2. Nitrogen transformations that may occur in deep vadose zone sediments. **(A)** Nitrogen and carbon concentrations and other sediment properties in site DH32. **(B)** Nitrogen and carbon concentrations and other sediment properties in site DH36. **(C)** Proposed mechanisms controlling nitrogen storage and transformation at the highlighted depths in (A) and (B). PW nitrate-N, pore water nitrate-N; TKN, total Kjeldahl nitrogen; EOC, hot-water extractable organic carbon; SOC, soil organic carbon; WFPS, water filled pore space; DNRA, dissimilatory nitrate reduction to ammonium; Anammox, anaerobic ammonium oxidation. See sediment texture in Figs. S4 and S5.

depths. In contrast, nitrate-N concentrations exhibited greater fluctuations among depths, likely due to greater mobility (Figs. S4–S30). Notably, we observed substantial ammonium-N accumulations in the deep vadose zone in two of the 27 sites (Figs. S4–S5). High ammonium-N concentrations at depths may indicate recent microbial N transformations in the vadose zone and were further elucidated by analyzing these two sites in detail.

Previous N mineralization and nitrification may be indicated by spikes of ammonium and nitrate concentrations at a depth of 19 m (Fig. 2A). Since N mineralization primarily depends on the available organic substrate (Wu et al., 2021), mineralization could be supported by substantial SOC and SON accumulations at 19 m depth, and co-occurs with sufficient moisture content. With the presence of organic C and N sources, the increases in $\delta^{13}C$ value and EOC concentration suggest the potential for intensive microbial processing and mineralization of SOC at the 19 m depth. The EOC can be used as a readily available energy source for soil microbes to mineralize the SON for N demands (Li et al., 2019), during which ammonium can be released (Fig. 2C). Increased ammonium concentration subsequently contributes to nitrification and thus nitrate concentration. While denitrification can occur under anaerobic conditions, nitrification should be the dominant process with a water filled pore space (WFPS) of 78 % and the sandy soil texture at this depth (Fig. S4). Even at 100 % WFPS, nitrification has been reported to be the dominant process of N_2O production in sandy soil (Pihlatie et al., 2004).

The relatively lower $\delta^{13}C$ value at the 12 m depth is not consistent with intensive mineralization despite the spikes of ammonium and EOC concentrations (Fig. 2B). Subsurface ammonium may form and accumulate at this depth due to the clayey soil texture (Fig. S5) since ammonium enrichment capacity increases with clay content (Fan et al., 2021). Unexpectedly, nitrate concentration did not increase with the increase of ammonium concentration in clay-rich sediments at this depth. Low nitrate concentration at depth suggests denitrification may have occurred and would be consistent with a high WFPS of 91 %. Even at the same WFPS, clay soil can have higher denitrification than sandy soil due to the formation of anaerobic microenvironments because of smaller pore sizes (Pihlatie et al., 2004). The increased EOC can further enhance denitrification since denitrification in deep vadose zone is usually limited by C availability (Chen et al., 2018; Peterson et al., 2013). Increased EOC might also partly support dissimilatory nitrate reduction to ammonium (DNRA) (Friedl et al., 2018) as microbes capable of DNRA would require a higher ratio of labile C to nitrate (EOC/nitrate-N, Fig. 2B) (Chutivisut et al., 2018). Anammox may also be possible at this depth as DNRA can also promote the transformation of N and occurrence of anammox in the vadose zone (Li et al., 2022).

There is a strong possibility for microbial N transformations in deep vadose zone, which can be controlled by labile C availability, soil water content, and soil texture (Fig. 2C). Our study demonstrated the critical role of vadose zone thickness, C availability, and soil texture in N storage and transformation. Our data show the critical need for additional work involving deep soil coring to better predict the occurrence of subsurface inorganic and organic N and C, transient storage, and subsequent transformation in the deep vadose zone to better assess potential groundwater contamination risks.

CRediT authorship contribution statement

Lidong Li: Conceptualization, Visualization, Formal analysis, Writing—original draft preparation.

Jordan Shields: Investigation, Methodology, Data curation, Validation, Formal analysis, Writing—reviewing.

Daniel D. Snow: Methodology, Funding acquisition, Supervision, Data curation, Resources, Validation, Project administration, Writing—reviewing and editing.

Michael Kaiser: Methodology, Visualization, Formal analysis, Writing—reviewing and editing.

Arindam Malakar: Conceptualization, Visualization, Methodology, Supervision, Resources, Project administration, Writing—reviewing and editing.

Data availability Data will be made available on request.

Competing interest The authors declare that they have no known competing financial interests or personal relationships that could have appeared to influence the work reported in this paper.

Acknowledgments Authors thank Water Sciences Laboratory (https://watercenter.unl.edu/water-sciences-laboratory2) for all analytical support reported in the study. The Central Platte Natural Resources District, Nebraska supported this work, grant number 92445, awarded to Snow. Malakar thanks USDA NIFA Grant (Accession No: 1027886).

References

Ascott, M., Gooddy, D.C., Wang, L., Stuart, M.E., Lewis, M., Ward, R., et al., 2017. Global patterns of nitrate storage in the vadose zone. Nat. Commun. 8, 1–7.

Burow, K.R., Nolan, B.T., Rupert, M.G., Dubrovsky, N.M., 2010. Nitrate in groundwater of the United States, 1991–2003. Environ. Sci. Technol. 44, 4988–4997.

Chen, S., Wang, F., Zhang, Y., Qin, S., Wei, S., Wang, S., et al., 2018. Organic carbon availability limiting microbial denitrification in the deep vadose zone. Environ. Microbiol. 20, 980–992.

Chutivisut, P., Isobe, K., Powtongsook, S., Pungrasmi, W., Kurisu, F., 2018. Distinct microbial community performing dissimilatory nitrate reduction to ammonium (DNRA) in a high C/NO_3–reactor. Microbes Environ. ME17193. 33, 264–271.

Exner, M.E., Hirsh, A.J., Spalding, R.F., 2014. Nebraska's groundwater legacy: nitrate contamination beneath irrigated cropland. Water Resour. Res. 50, 4474–4489.

Fan, X., Xue, Q., Liu, S., Tang, J., Qiao, J., Huang, Y., et al., 2021. The influence of soil particle size distribution and clay minerals on ammonium nitrogen in weathered crust elution-deposited rare earth tailing. Ecotoxicol. Environ. Saf. 208, 111663.

Friedl, J., De Rosa, D., Rowlings, D.W., Grace, P.R., Müller, C., Scheer, C., 2018. Dissimilatory nitrate reduction to ammonium (DNRA), not denitrification dominates nitrate reduction in subtropical pasture soils upon rewetting. Soil Biol. Biochem. 125, 340–349.

Jia, X., Zhu, Y., Huang, L., Wei, X., Fang, Y., Wu, L., et al., 2018. Mineral N stock and nitrate accumulation in the 50 to 200 m profile on the loess plateau. Sci. Total Environ. 633, 999–1006.

Juntakut, P., Snow, D.D., Haacker, E.M., Ray, C., 2019. The long term effect of agricultural, vadose zone and climatic factors on nitrate contamination in Nebraska's groundwater system. J. Contam. Hydrol. 220, 33–48.

Kettler, T., Doran, J.W., Gilbert, T., 2001. Simplified method for soil particle-size determination to accompany soil-quality analyses. Soil Sci. Soc. Am. J. 65, 849–852.

Li, H., Liang, S., Chi, Z., Wu, H., Yan, B., 2022. Unveiling microbial community and function involved in anammox in paddy vadose under groundwater irrigation. Sci. Total Environ. 849, 157876.

Li, L., Wilson, C.B., He, H., Zhang, X., Zhou, F., Schaeffer, S.M., 2019. Physical, biochemical, and microbial controls on amino sugar accumulation in soils under long-term cover cropping and no-tillage farming. Soil Biol. Biochem. 135, 369–378.

Mekala, C., Nambi, I.M., 2017. Understanding the hydrologic control of N cycle: effect of water filled pore space on heterotrophic nitrification, denitrification and dissimilatory nitrate reduction to ammonium mechanisms in unsaturated soils. J. Contam. Hydrol. 202, 11–22.

Peterson, M., Curtin, D., Thomas, S., Clough, T., Meenken, E., 2013. Denitrification in vadose zone material amended with dissolved organic matter from topsoil and subsoil. Soil Biol. Biochem. 61, 96–104.

Pihlatie, M., Syväsalo, E., Simojoki, A., Esala, M., Regina, K., 2004. Contribution of nitrification and denitrification to N_2O production in peat, clay and loamy sand soils under different soil moisture conditions. Nutr. Cycl. Agroecosyst. 70, 135–141.

Voisin, J., Cournoyer, B., Vienney, A., Mermillod-Blondin, F., 2018. Aquifer recharge with stormwater runoff in urban areas: influence of vadose zone thickness on nutrient and bacterial transfers from the surface of infiltration basins to

groundwater. Sci. Total Environ. 637, 1496–1507.
Wang, S., Radny, D., Huang, S., Zhuang, L., Zhao, S., Berg, M., et al., 2017. Nitrogen loss by anaerobic ammonium oxidation in unconfined aquifer soils. Sci. Rep. 7, 1–10.
Weitzman, J.N., Brooks, J.R., Compton, J.E., Faulkner, B.R., Mayer, P.M., Peachey, R.E., et al., 2022. Deep soil nitrogen storage slows nitrate leaching through the vadose zone. Agric. Ecosyst. Environ. 332, 107949.
Wu, H., Cai, A., Xing, T., Huai, S., Zhu, P., Xu, M., et al., 2021. Fertilization enhances mineralization of soil carbon and nitrogen pools by regulating the bacterial community and biomass. J. Soils Sediments 21, 1633–1643.
Xin, J., Liu, Y., Chen, F., Duan, Y., Wei, G., Zheng, X., et al., 2019. The missing nitrogen pieces: a critical review on the distribution, transformation, and budget of nitrogen in the vadose zone-groundwater system. Water Res. 165, 114977.
Zhu, G., Wang, S., Li, Y., Zhuang, L., Zhao, S., Wang, C., et al., 2018. Microbial pathways for nitrogen loss in an upland soil. Environ. Microbiol. 20, 1723–1738.

Appendix A. Supplementary data

Supplementary data to this article follows.

The supplementary data contains additional figures (Fig. S1-S30) and tables (Tables S1-S3).

Fig. S1, shows sampling locations.

Fig. S2, shows soil composition of the study site;

Fig. S3, shows the soil sampling protocol;

Fig. S4, shows detailed depth profile of site DH-32, PW nitrate-N, pore water nitrate-N; TKN, total Kjeldahl nitrogen; EOC, hot-water extractable organic carbon; SOC, soil organic carbon; WFPS, water filled pore space.;

Fig. S5, shows the depth profile of Site DH-36, PW nitrate-N, pore water nitrate-N; TKN, total Kjeldahl nitrogen; EOC, hot-water extractable organic carbon; SOC, soil organic carbon; WFPS, water filled pore space.;

Fig. S6 to S30, shows depth profile of soil nitrate and ammonium of all other study sites;

Table S1, Site ID, coordinates, sampling dates, and rig type used for coring

Table S2, Description of location ground water quality phase, irrigation method, and self-reported crop type and fertilizer application rates, and

Table S3 Sampling depth and depth of water table. “Refusal” indicates that the water table was not reached.

Supplementary materials

Labile carbon and soil texture control nitrogen transformation in deep vadose zone

Lidong Li[1], Jordan Shields[2], Daniel D. Snow[2], Michael Kaiser[1], Arindam Malakar[2,] *

[1]University of Nebraska-Lincoln, Department of Agronomy and Horticulture, 1875 N 38th St, 279 Plant Sciences Hall, PO Box 830915, Lincoln, NE 68583-0915, USA.

[2]School of Natural Resources and Nebraska Water Center, part of the Robert B. Daugherty Water for Food Global Institute, University of Nebraska, Lincoln, NE, 68583-0844, USA.

*Corresponding author. Email: amalakar2@unl.edu

Figures S1 – S30

Tables S1 – S3

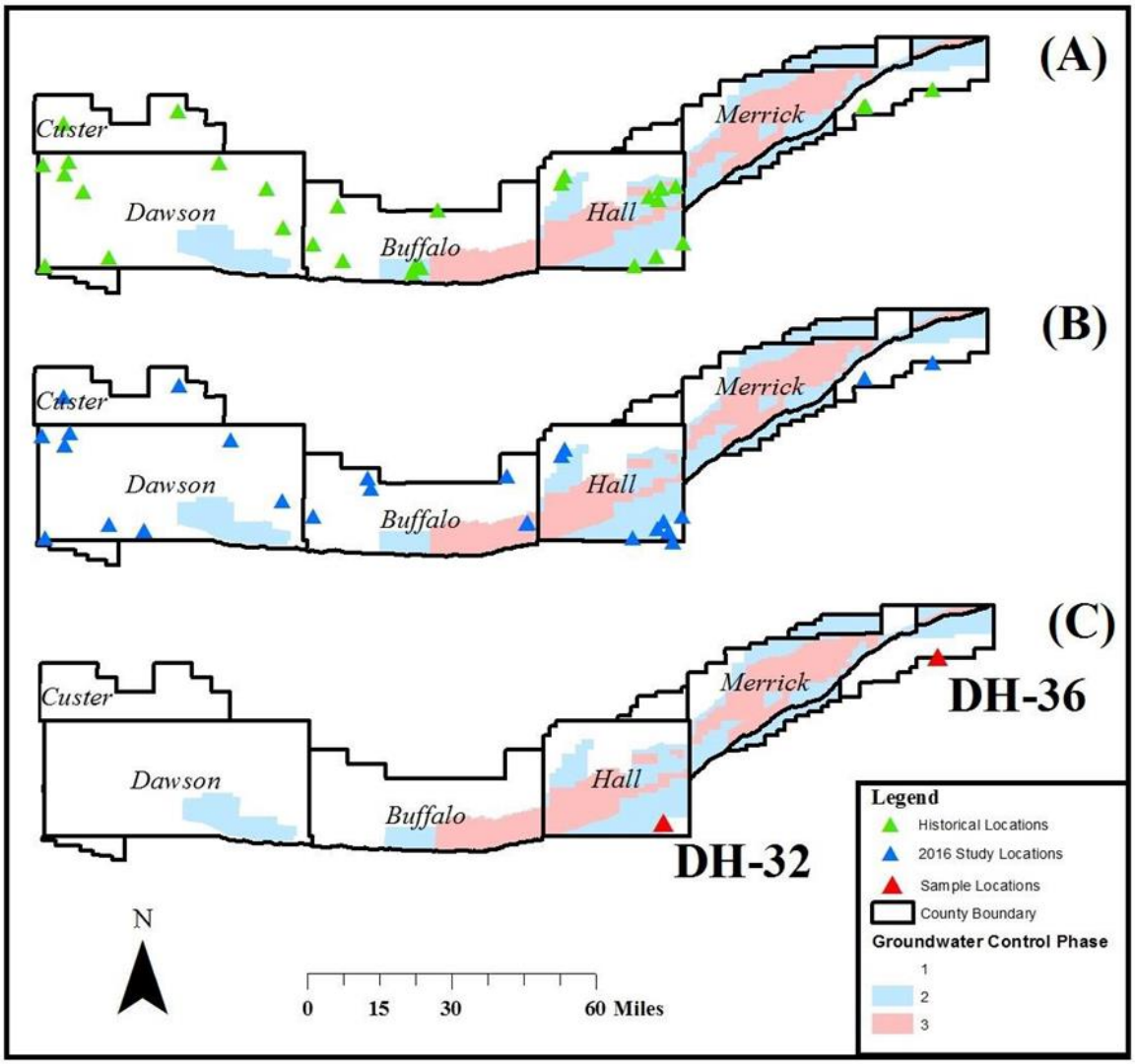

Fig. S1. Sampling locations from the Central Platte Natural Resource District. (A) the 1990's study, (B) the 2016 study, (C) two special locations.

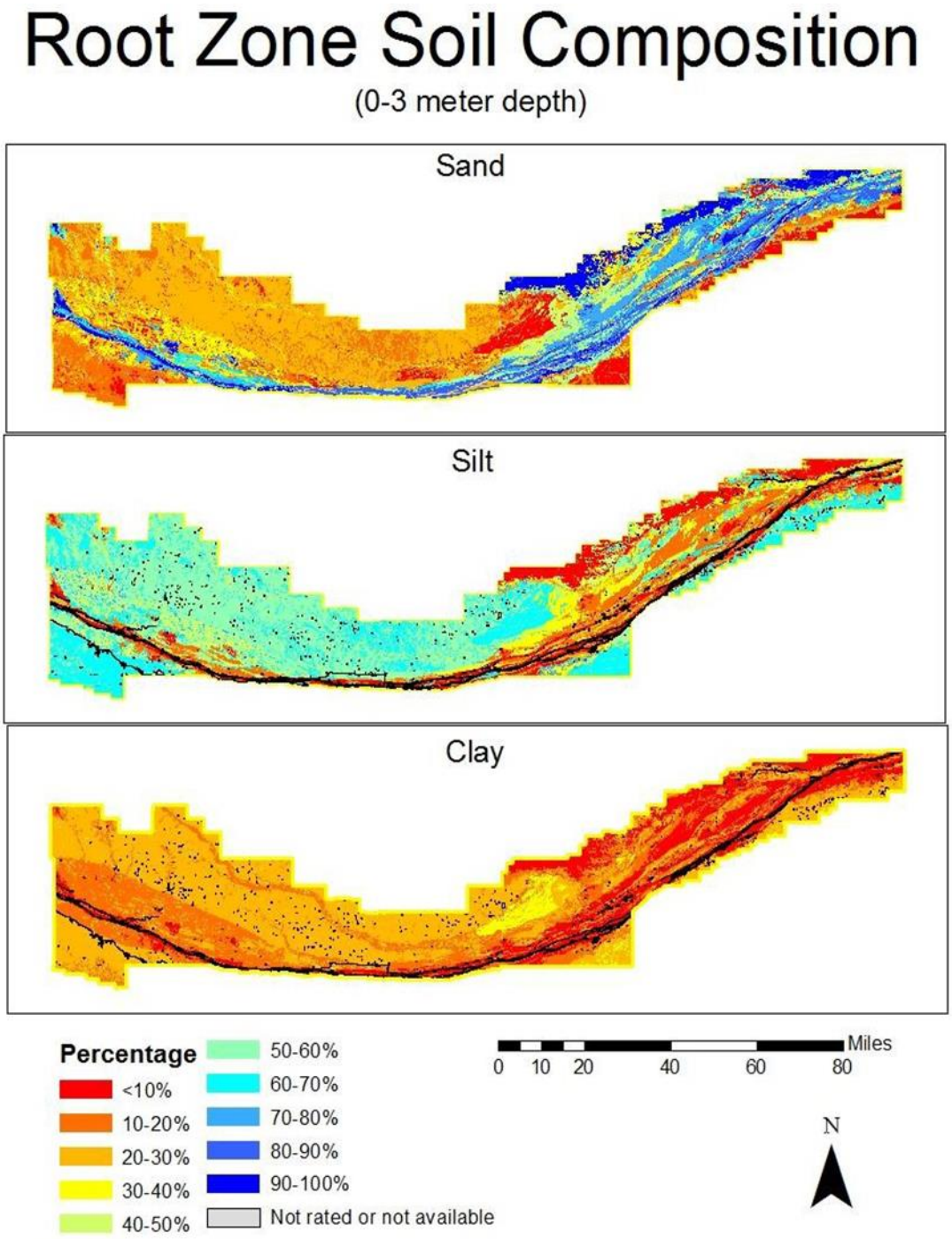

Fig. S2. Root zone soil composition as a percentage from the United States Department of Agriculture Natural Resource Conservation Service Soil Survey Geographic Database.

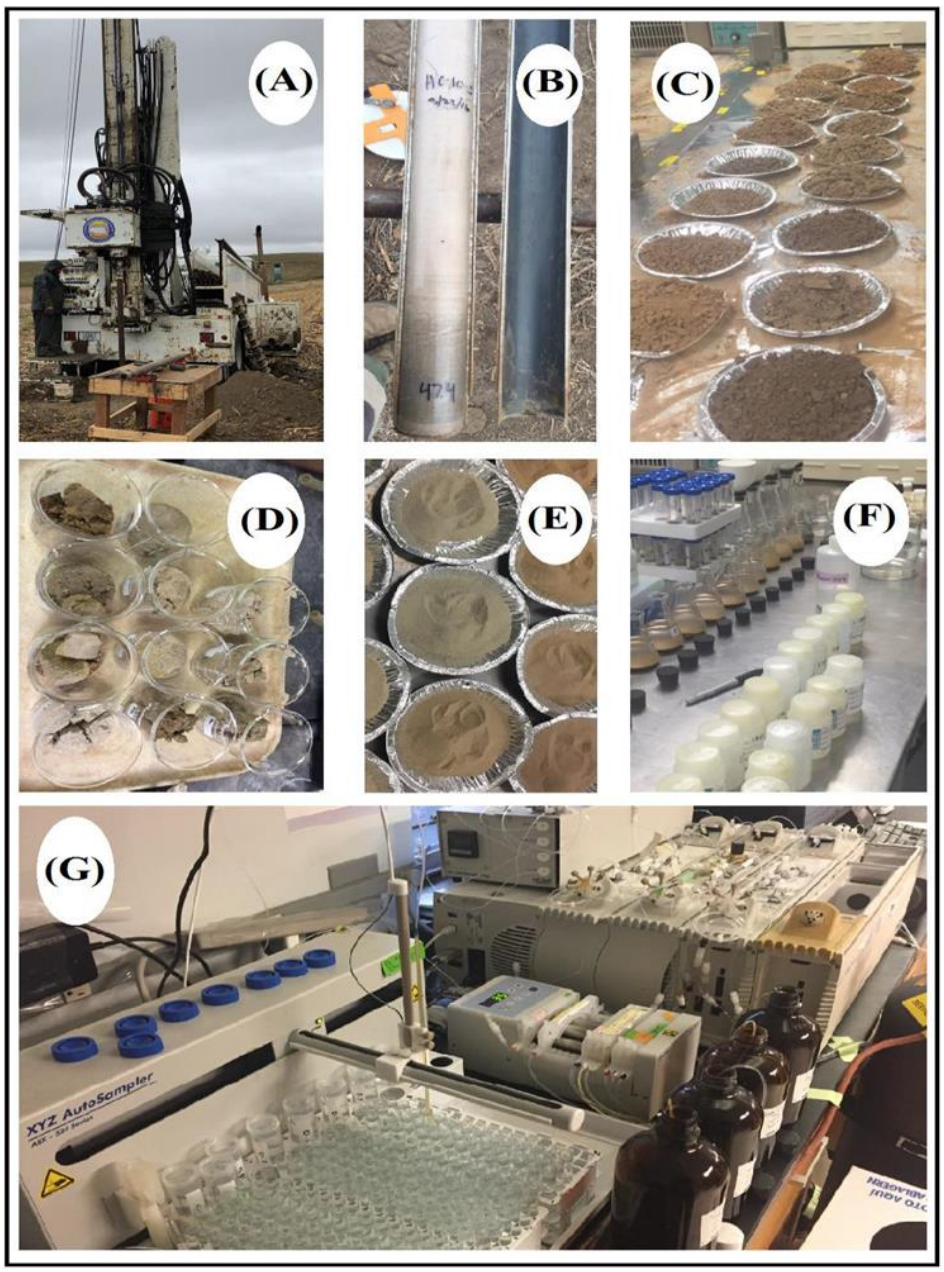

Fig. S3. (A) the drill rig used for coring (B) the split spoon core barrel with the acrylic liners to contain soil samples (C) soil cores had been broken down and homogenized based on changes in lithology (D) oven dried subsamples used for moisture content and bulk density measurements (E) homogenized, oven dried soil has been passed through a Willey Mill (F) samples after shaking in KCl solution for nitrate and ammonium extraction (G) KCl extracts being analyzed on a Lachat Quikchem 8500 FIA.

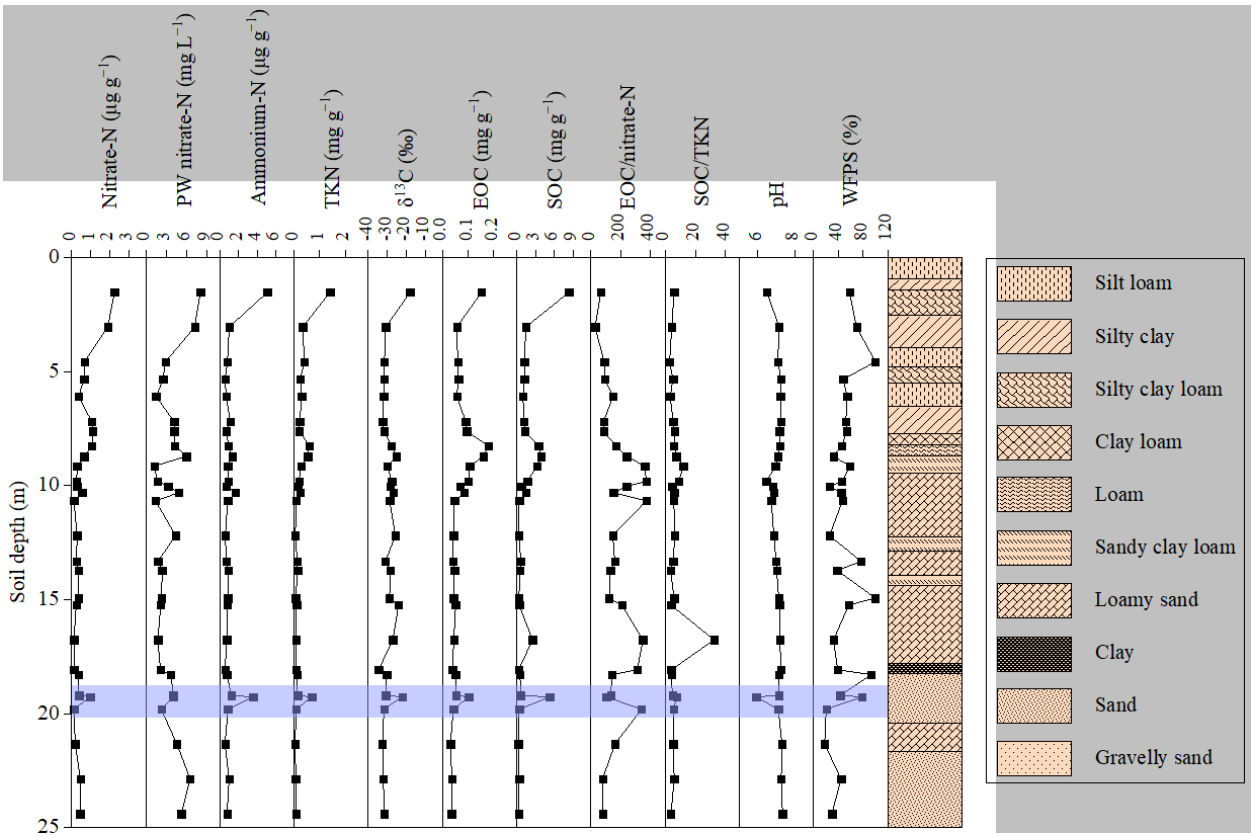

Fig. S4. Site DH-32. PW nitrate-N, pore water nitrate-N; TKN, total Kjeldahl nitrogen; EOC, hot-water extractable organic carbon; SOC, soil organic carbon; WFPS, water filled pore space.

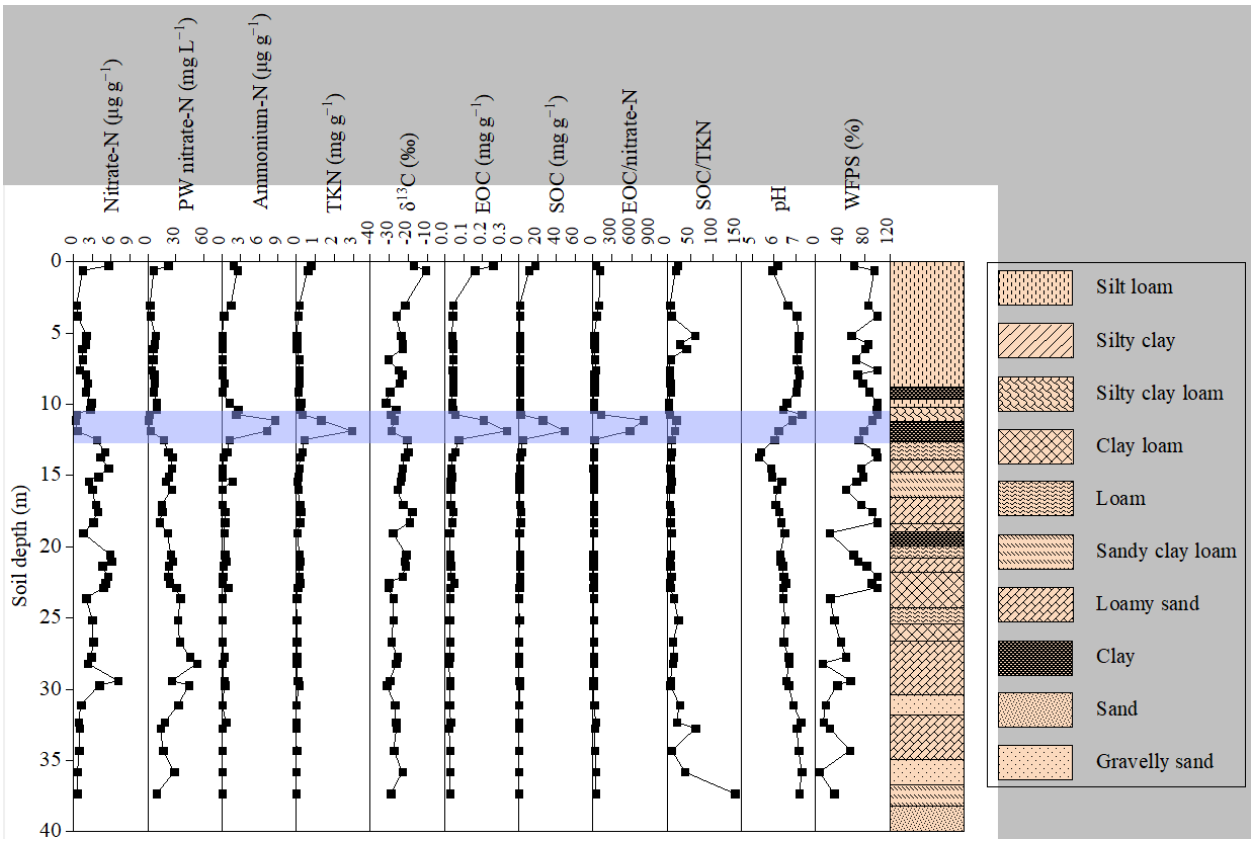

Fig. S5. Site DH-36. PW nitrate-N, pore water nitrate-N; TKN, total Kjeldahl nitrogen; EOC, hot-water extractable organic carbon; SOC, soil organic carbon; WFPS, water filled pore space.

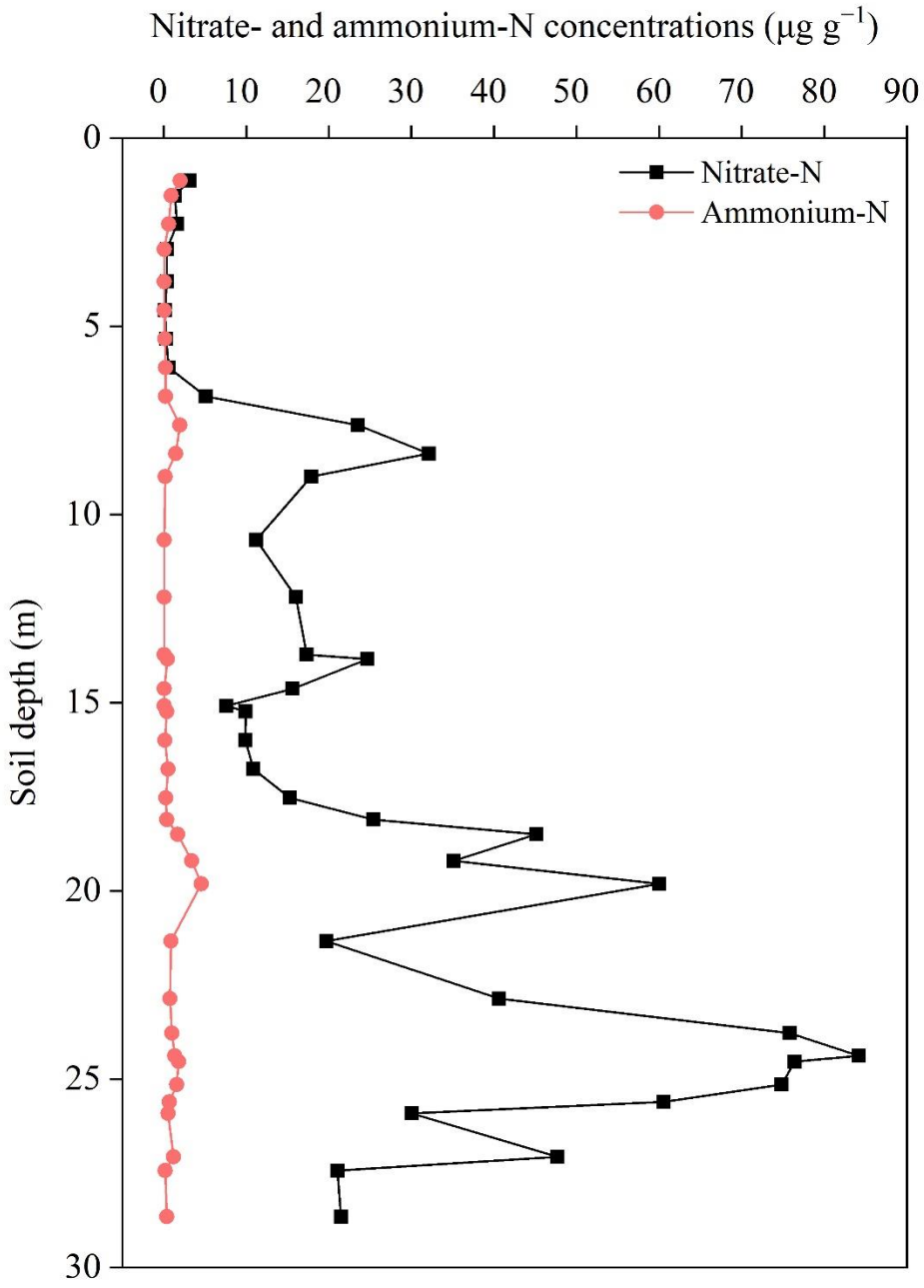

Fig. S6. Site DH-19.

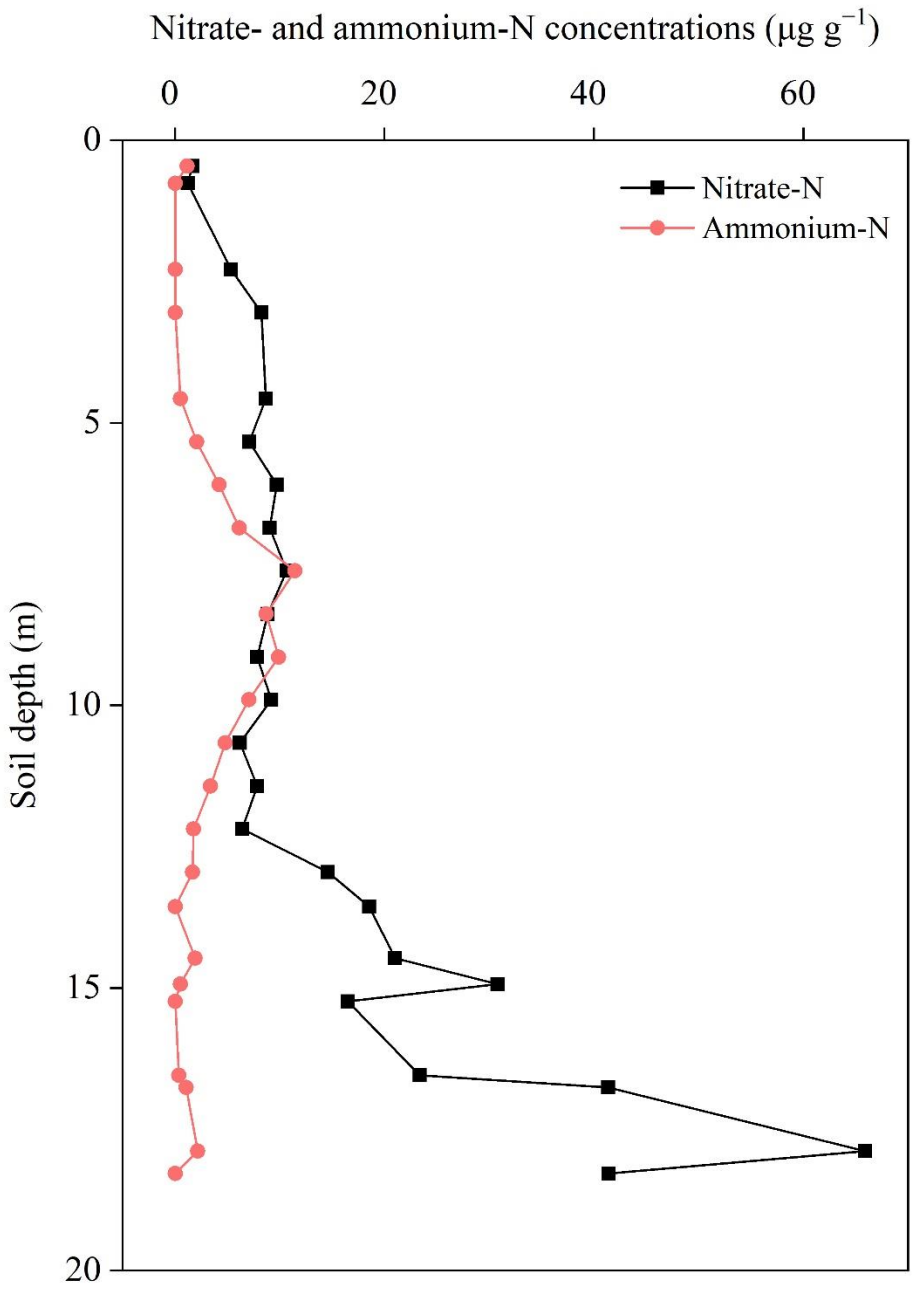

Fig. S7. Site DH-20.

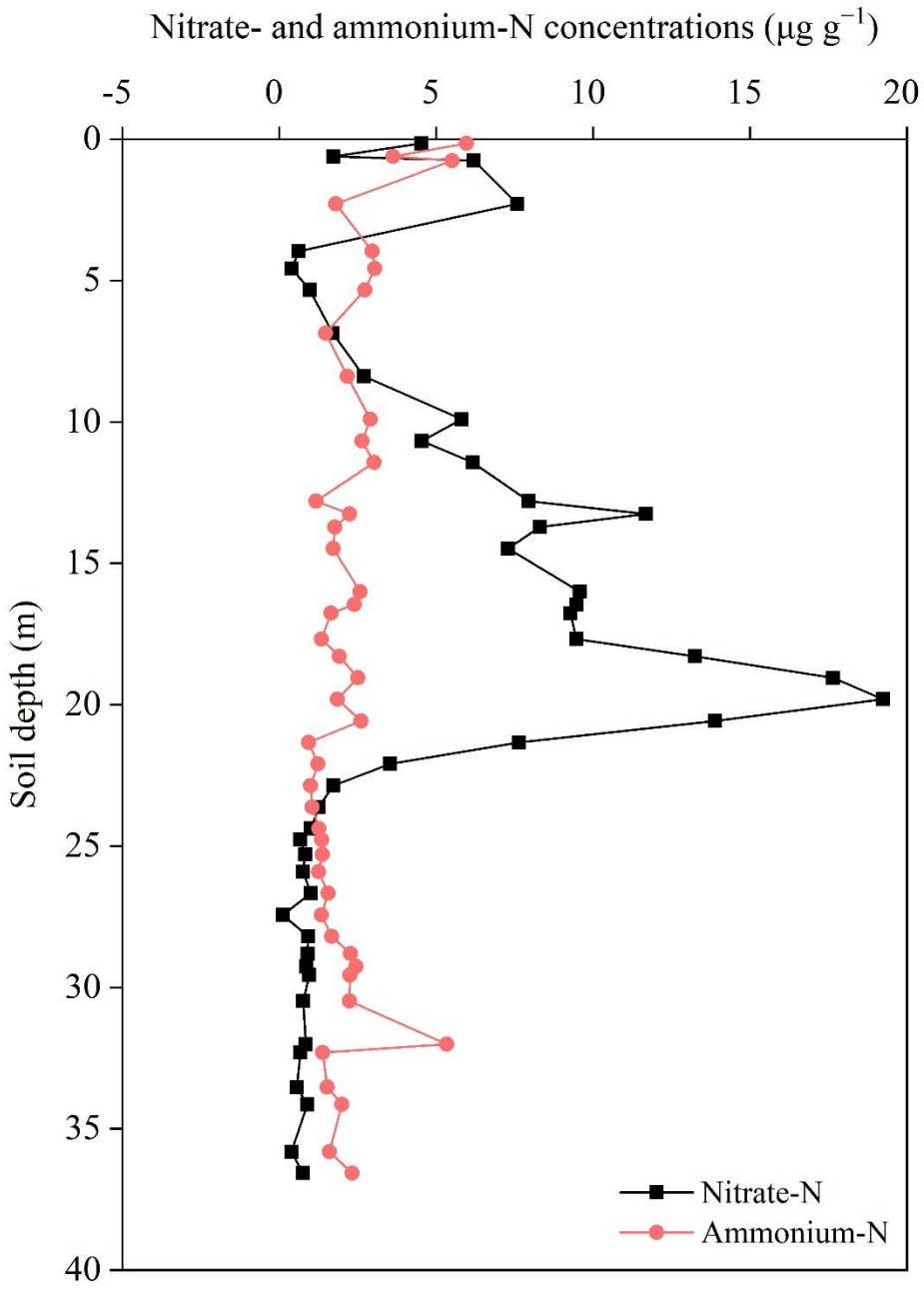

Fig. S8. Site DH-21.

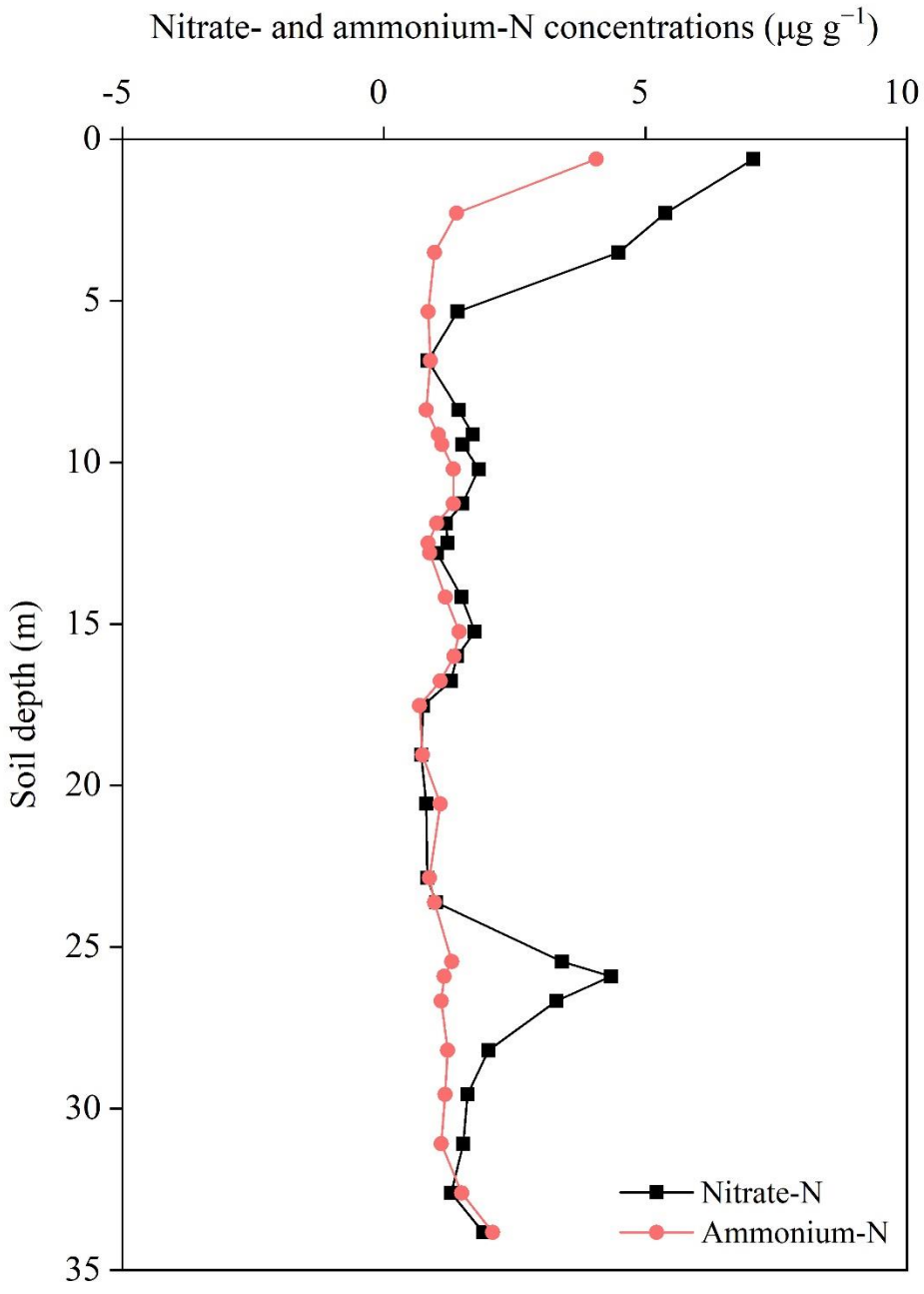

Fig. S9. Site DH-22.

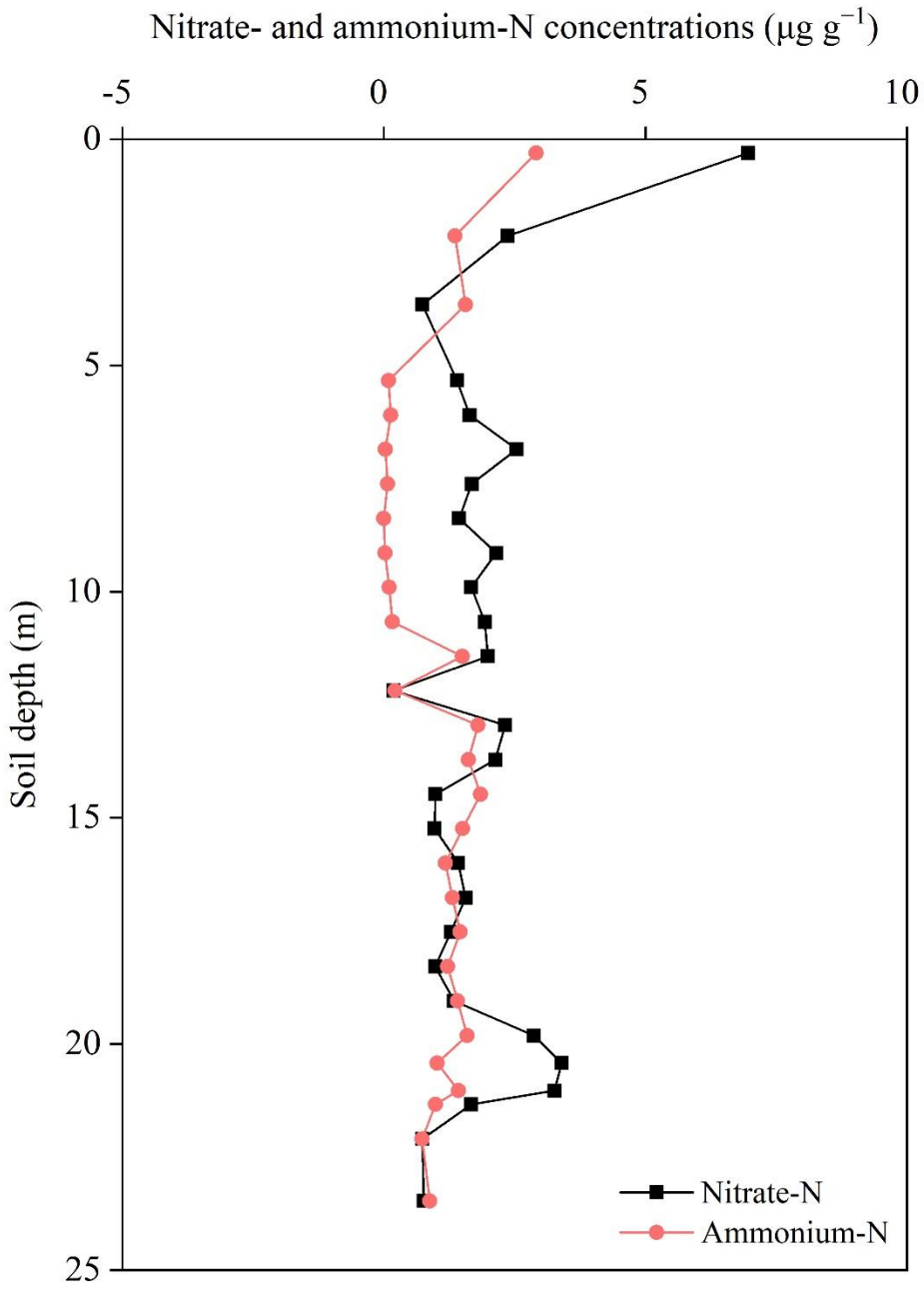

Fig. S10. Site DH-26.

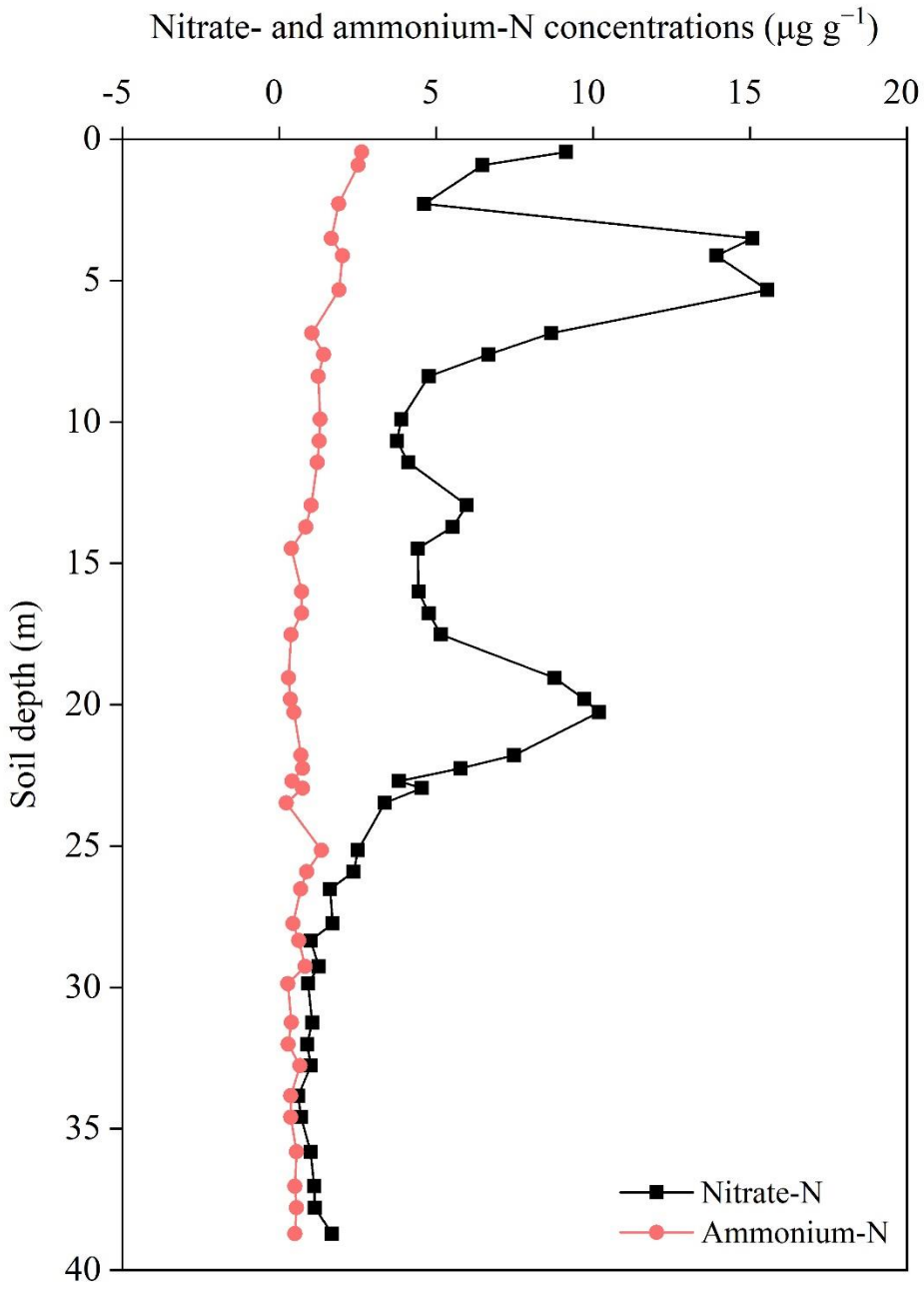

Fig. S11. Site DH-28.

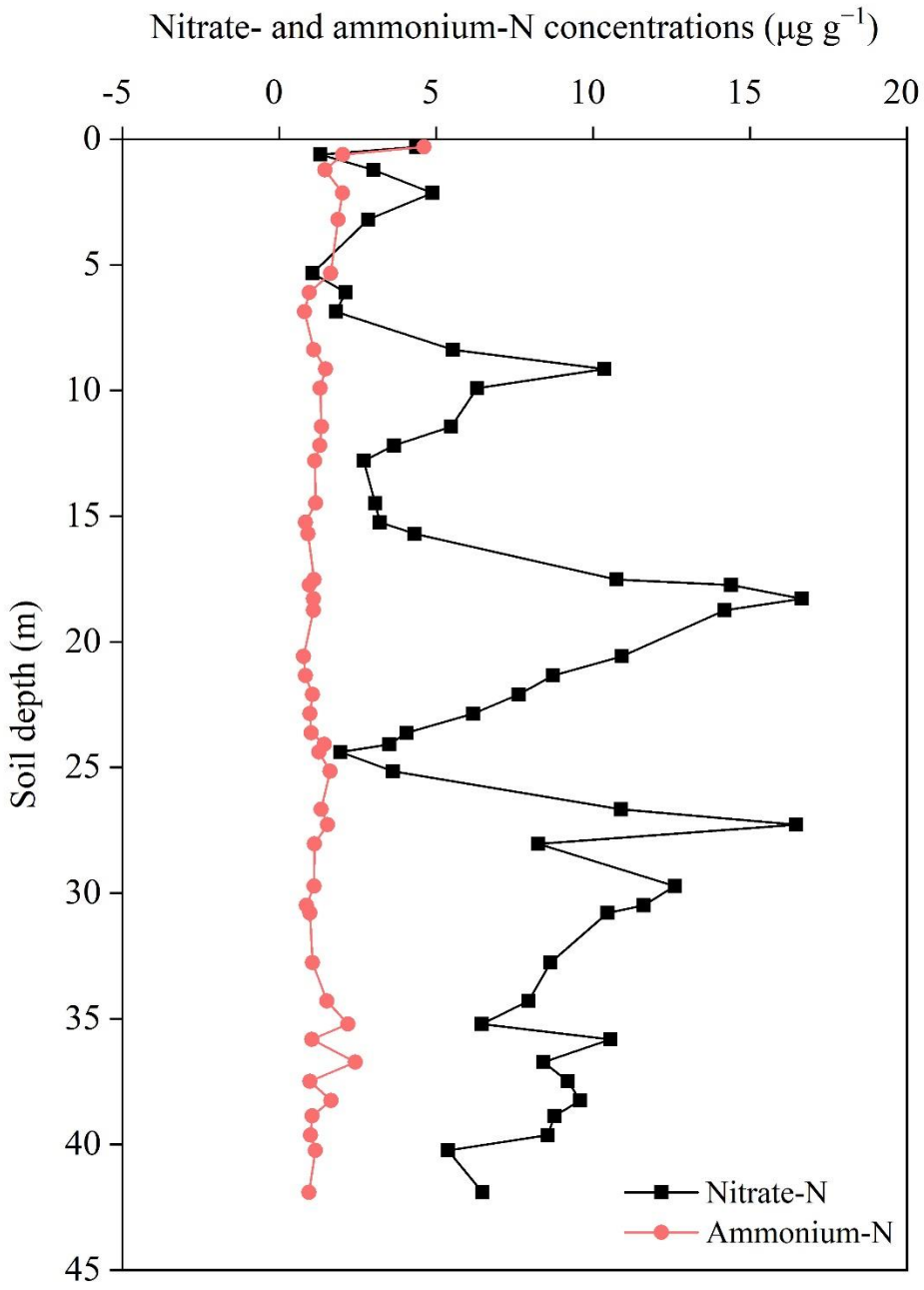

Fig. S12. Site DH-29.

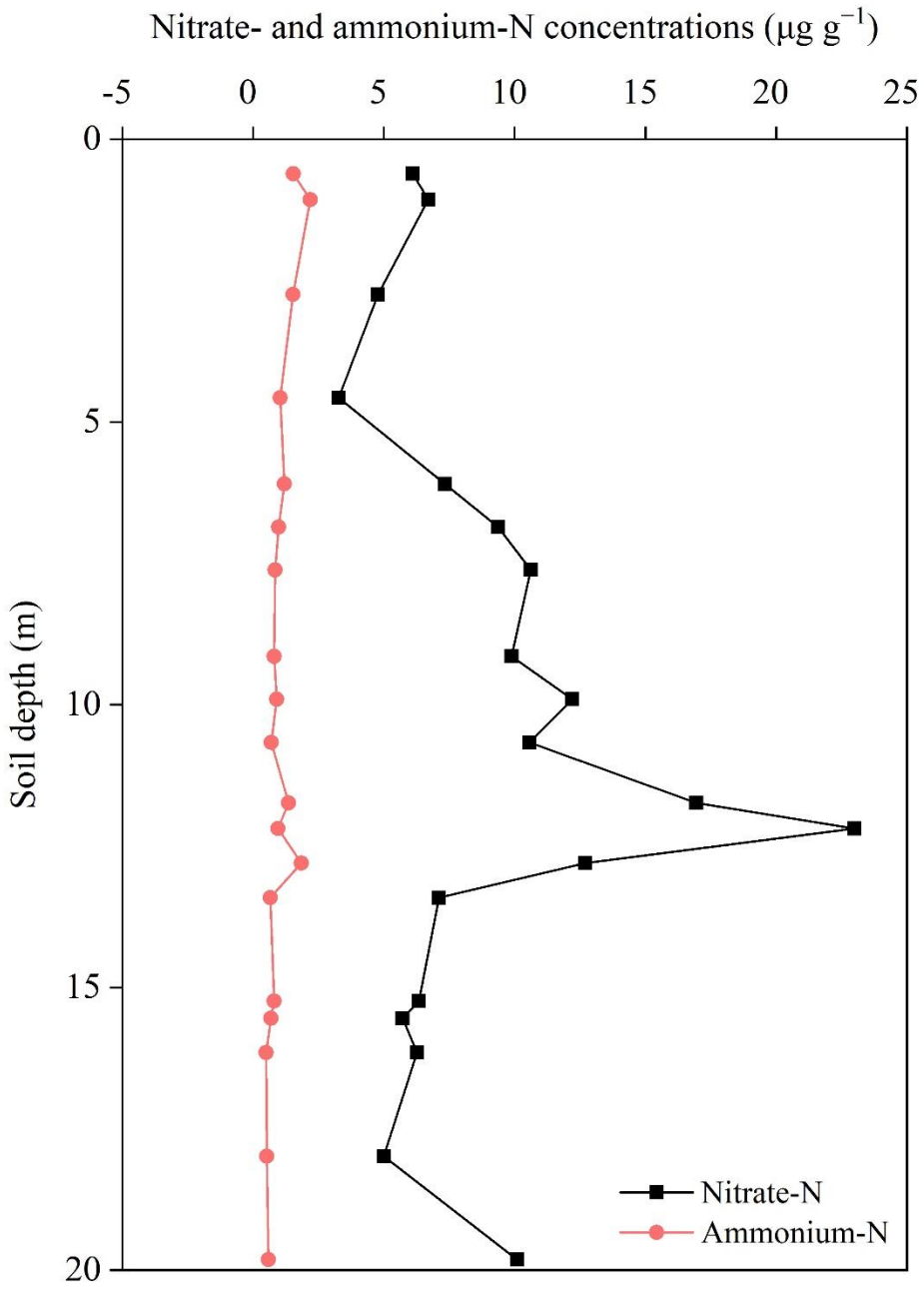

Fig. S13. Site DH-30.

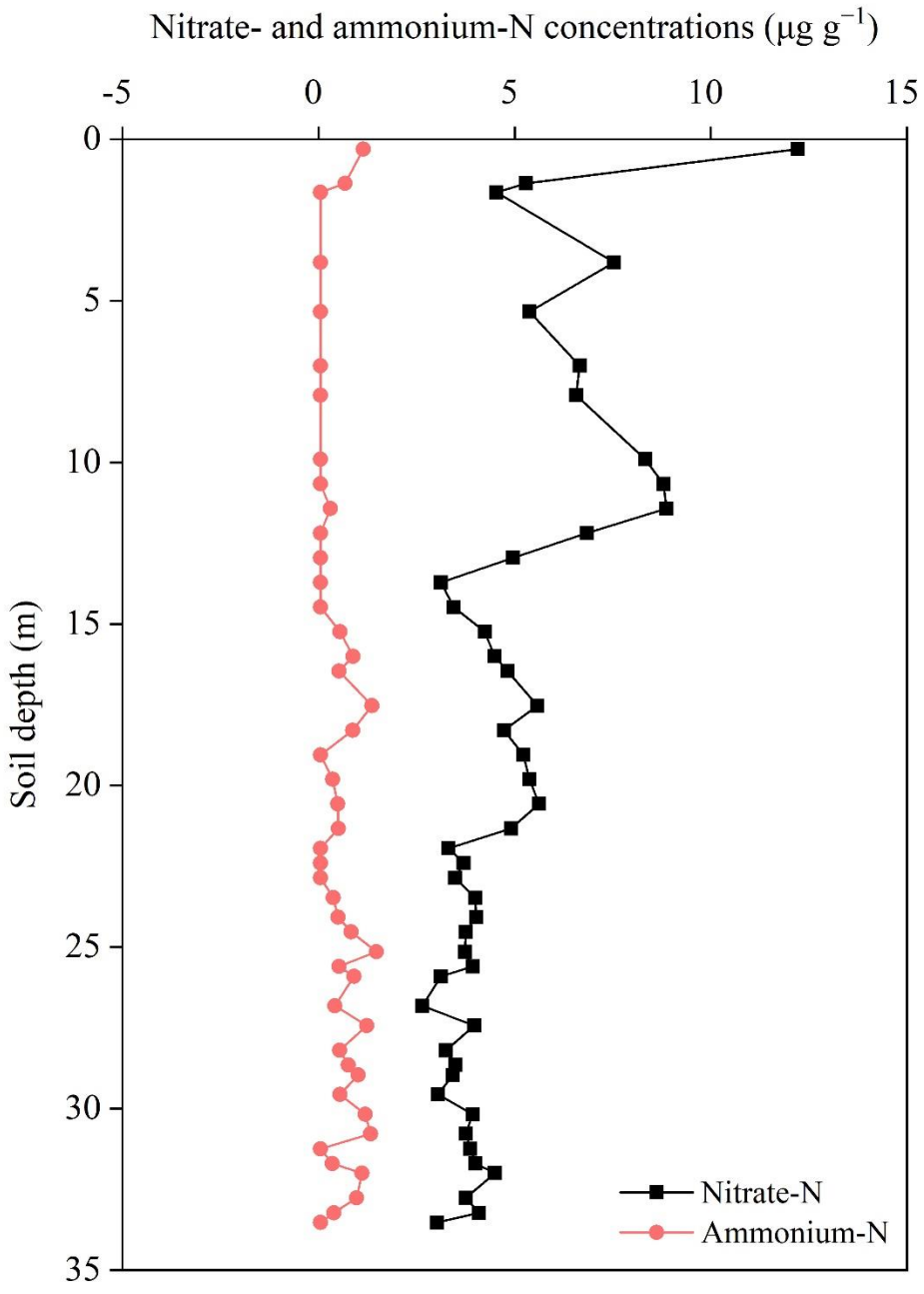

Fig. S14. Site DH-31.

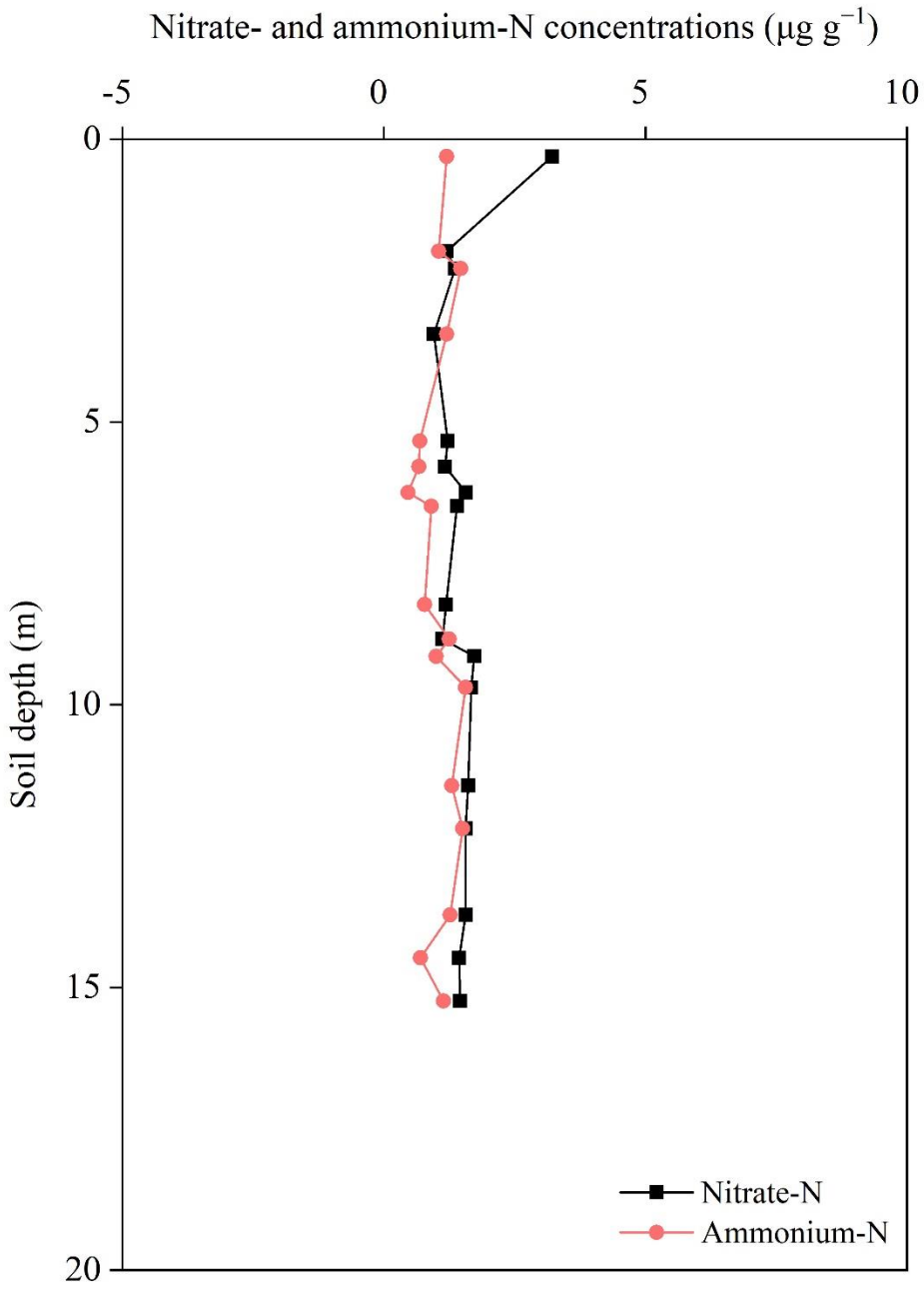

Fig. S15. Site DH-37.

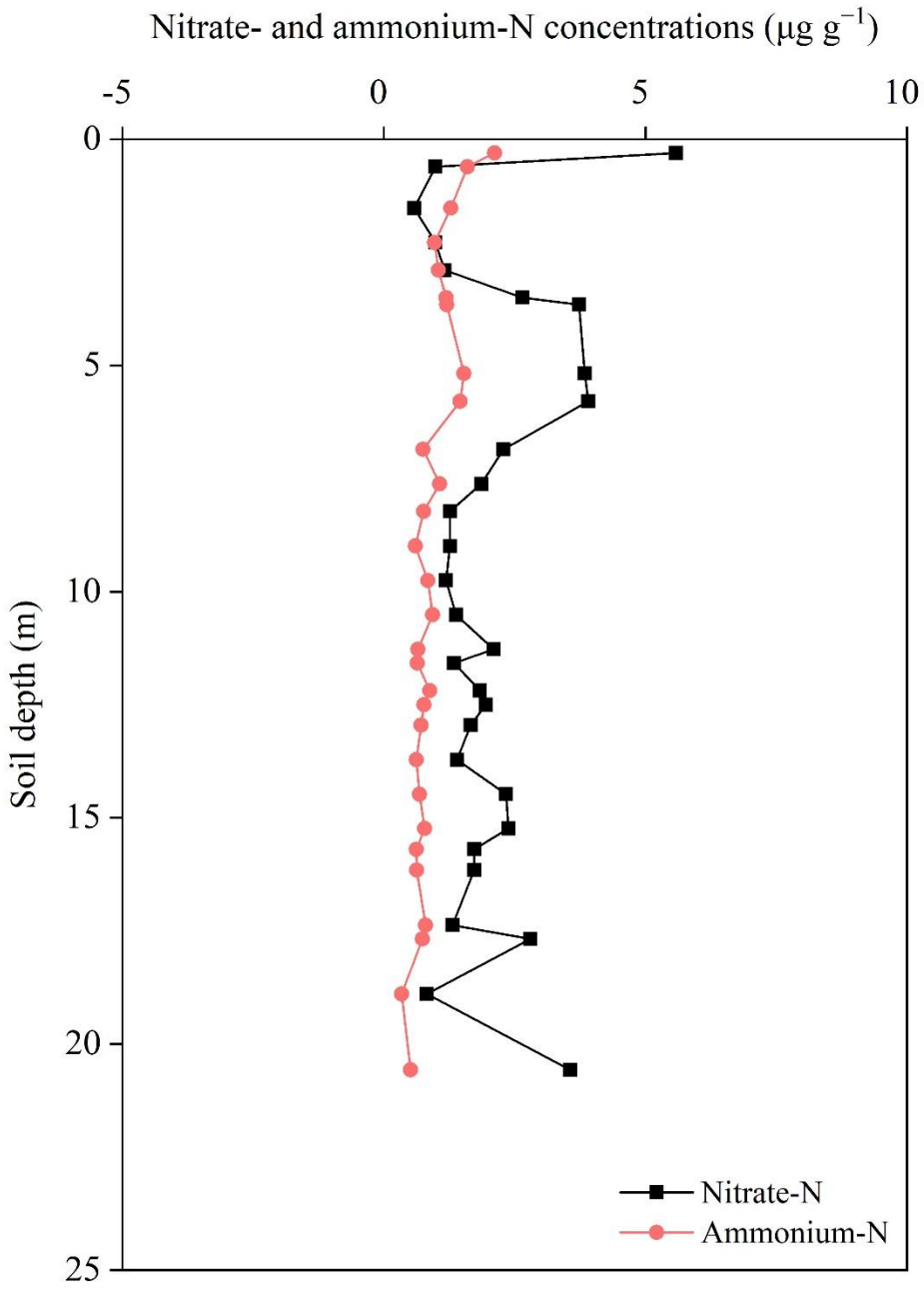

Fig. S16. Site DH-38.

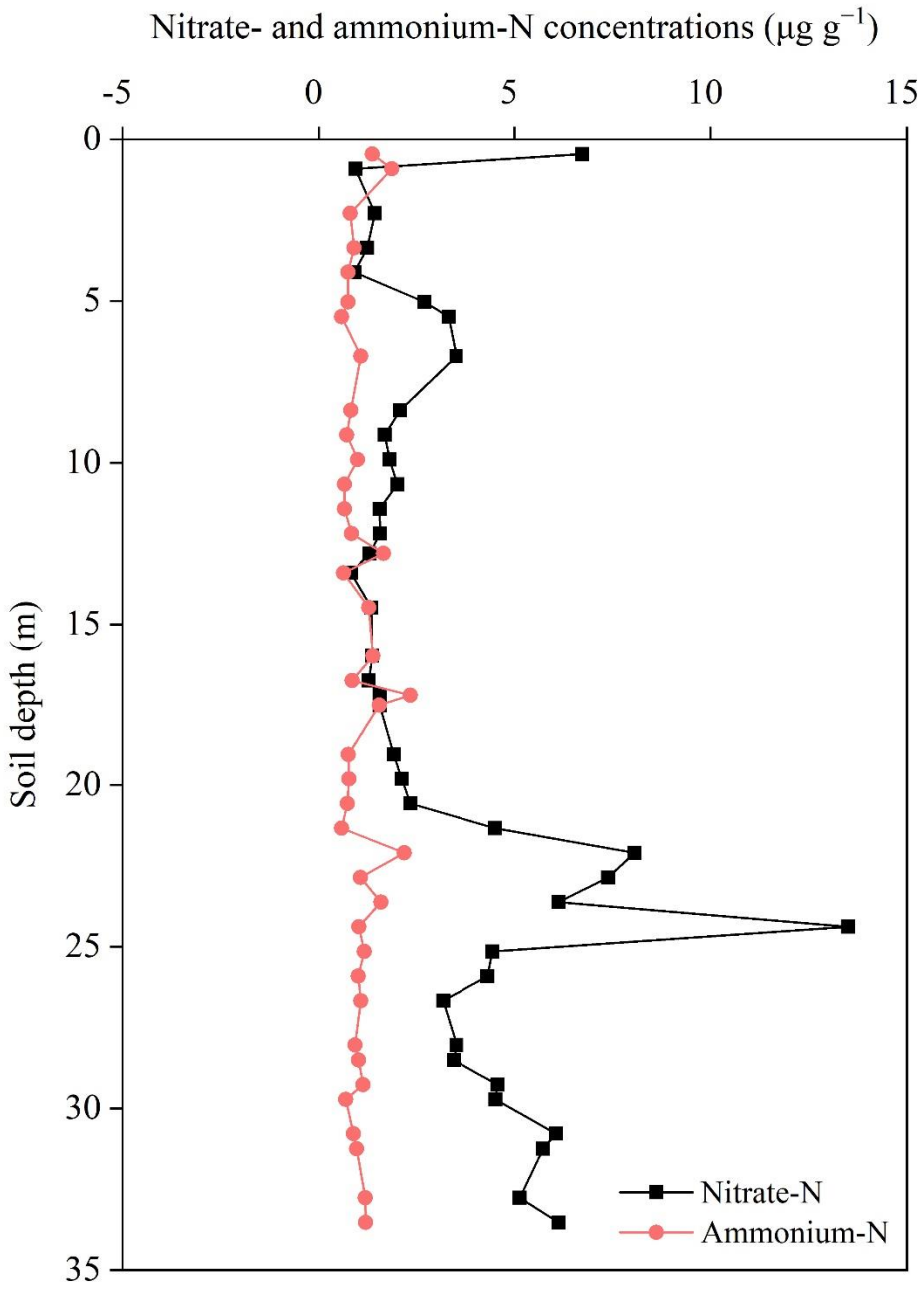

Fig. S17. Site DH-39.

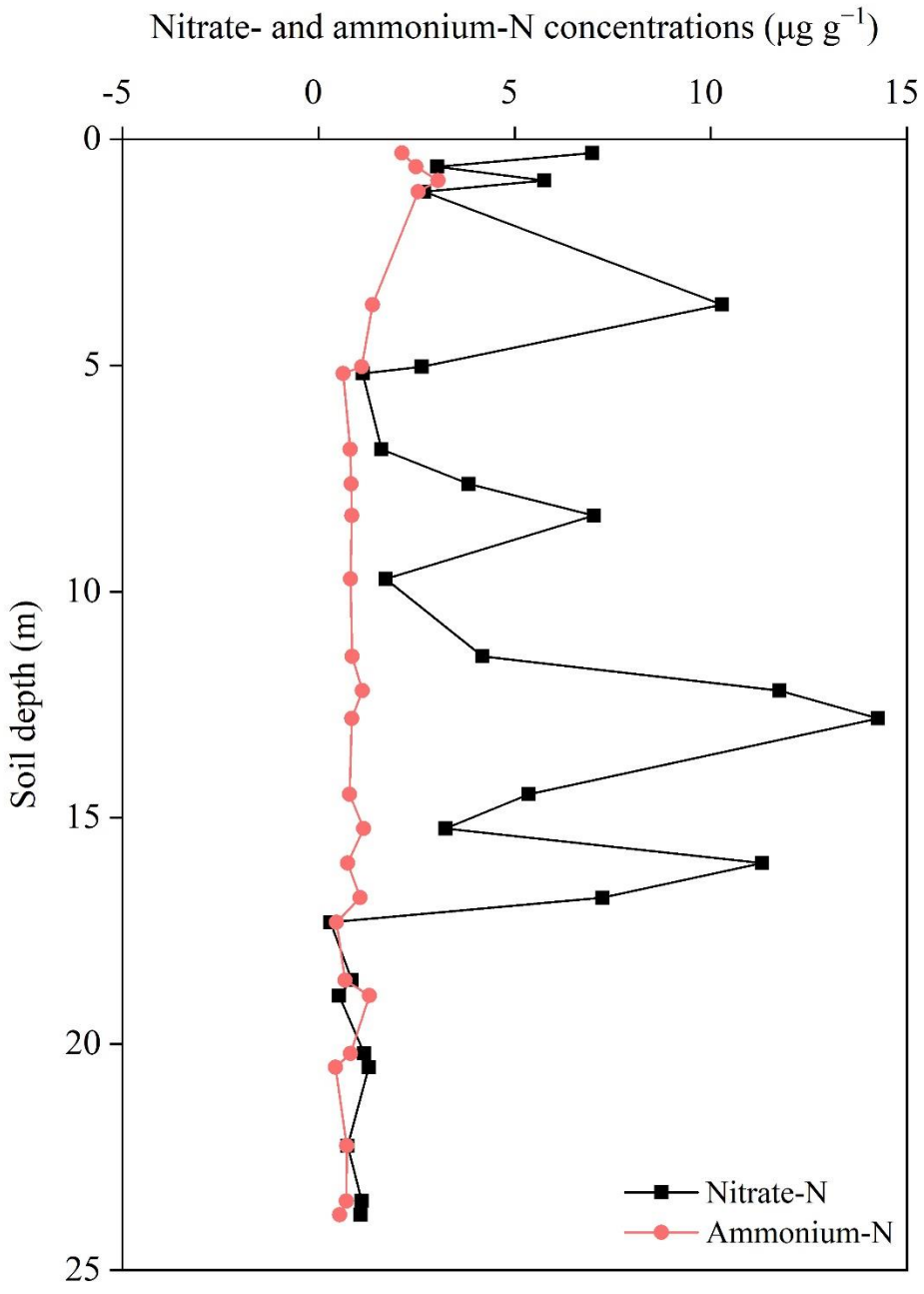

Fig. S18. Site DH-40.

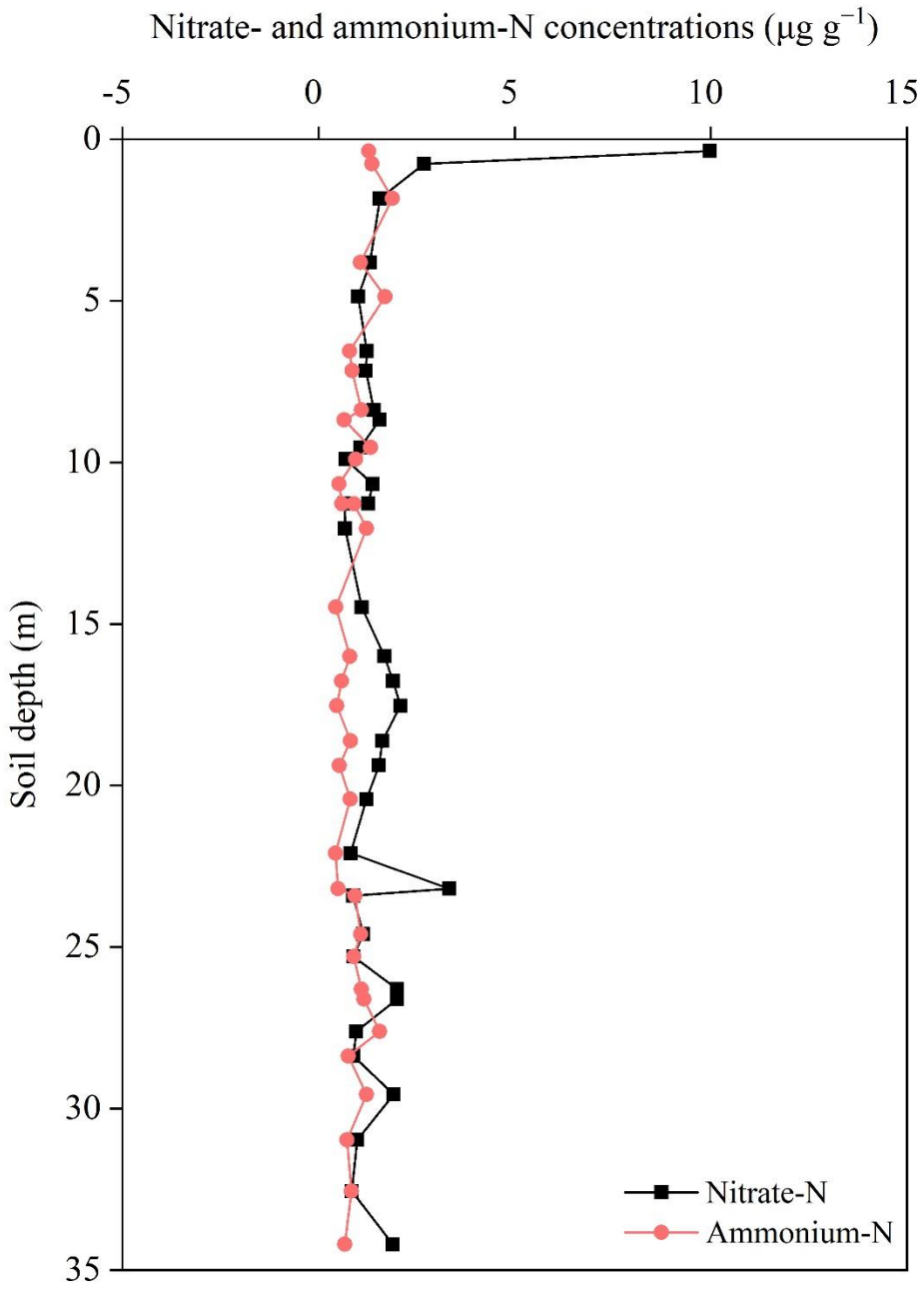

Fig. S19. Site DH-41.

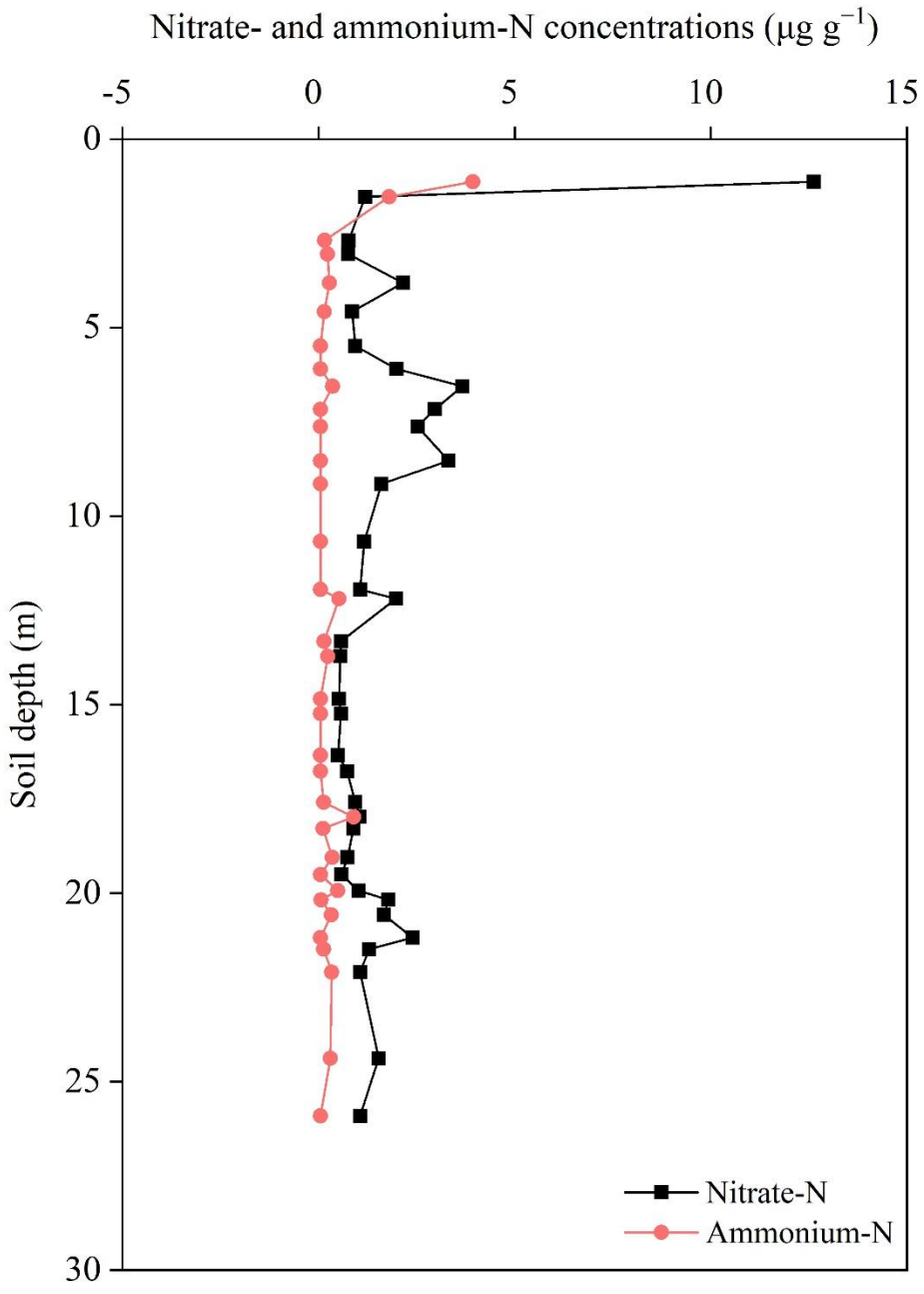

Fig. S20. Site DH-47.

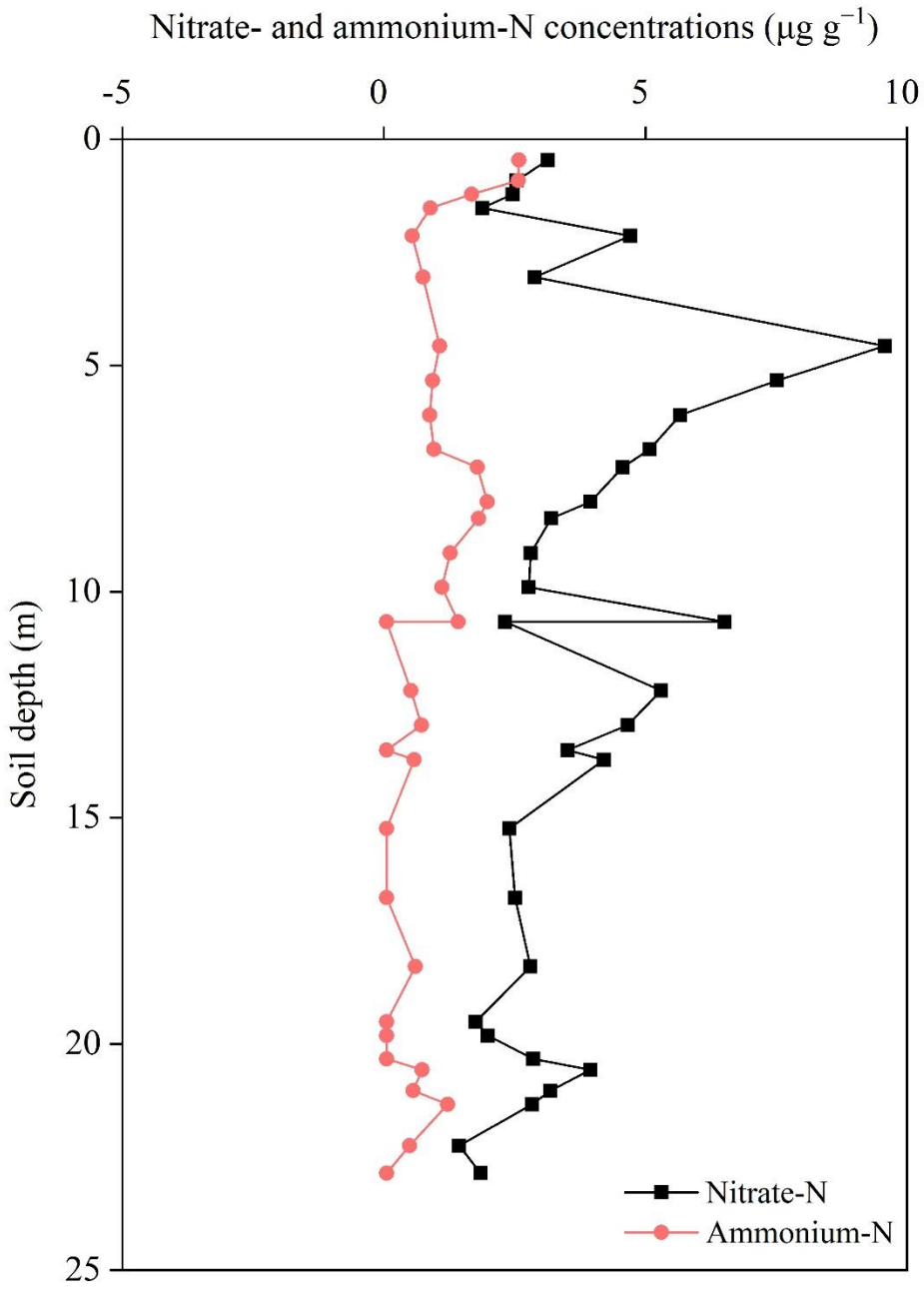

Fig. S21. Site DH-48.

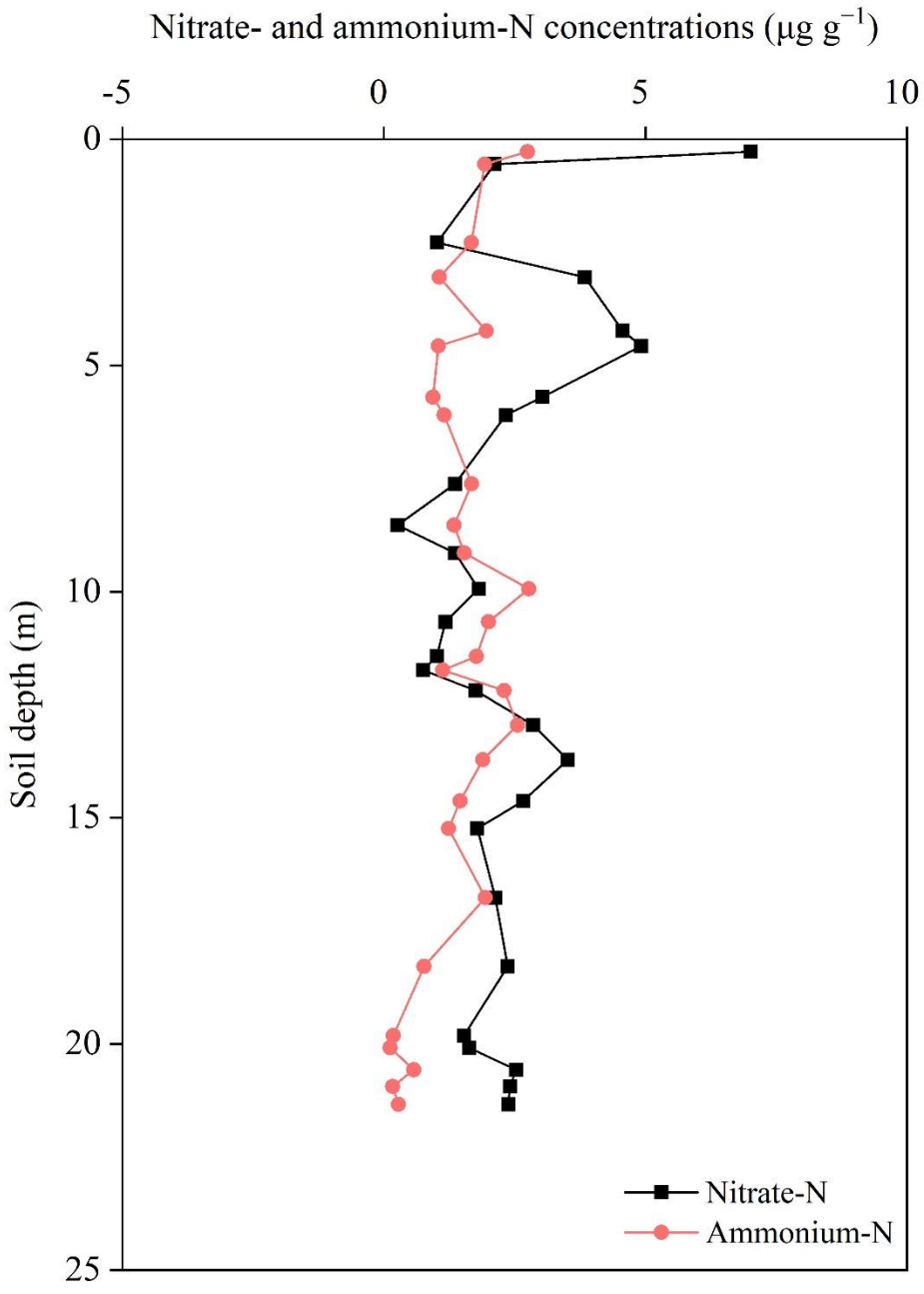

Fig. S22. Site DH-49.

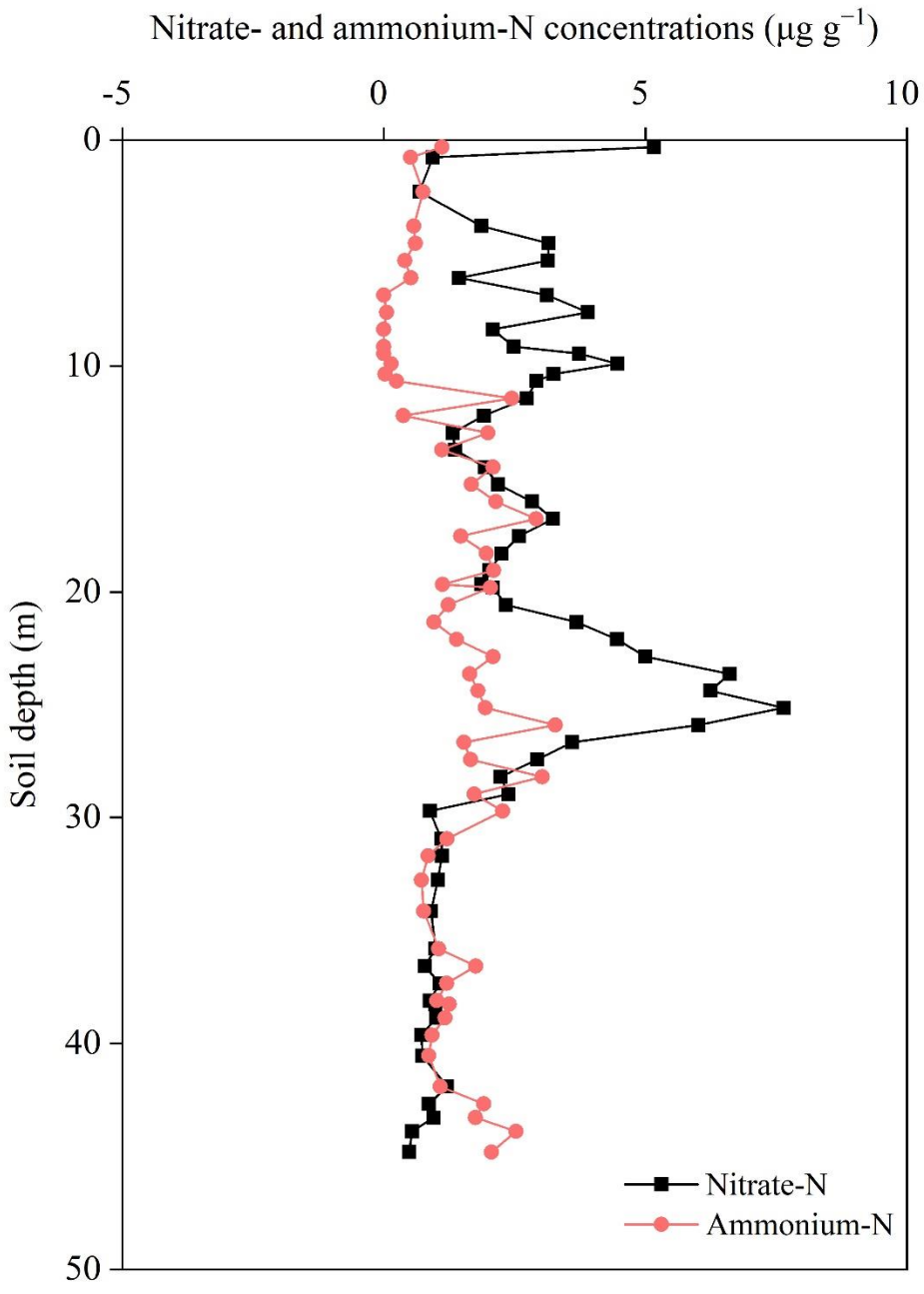

Fig. S23. Site DH-50.

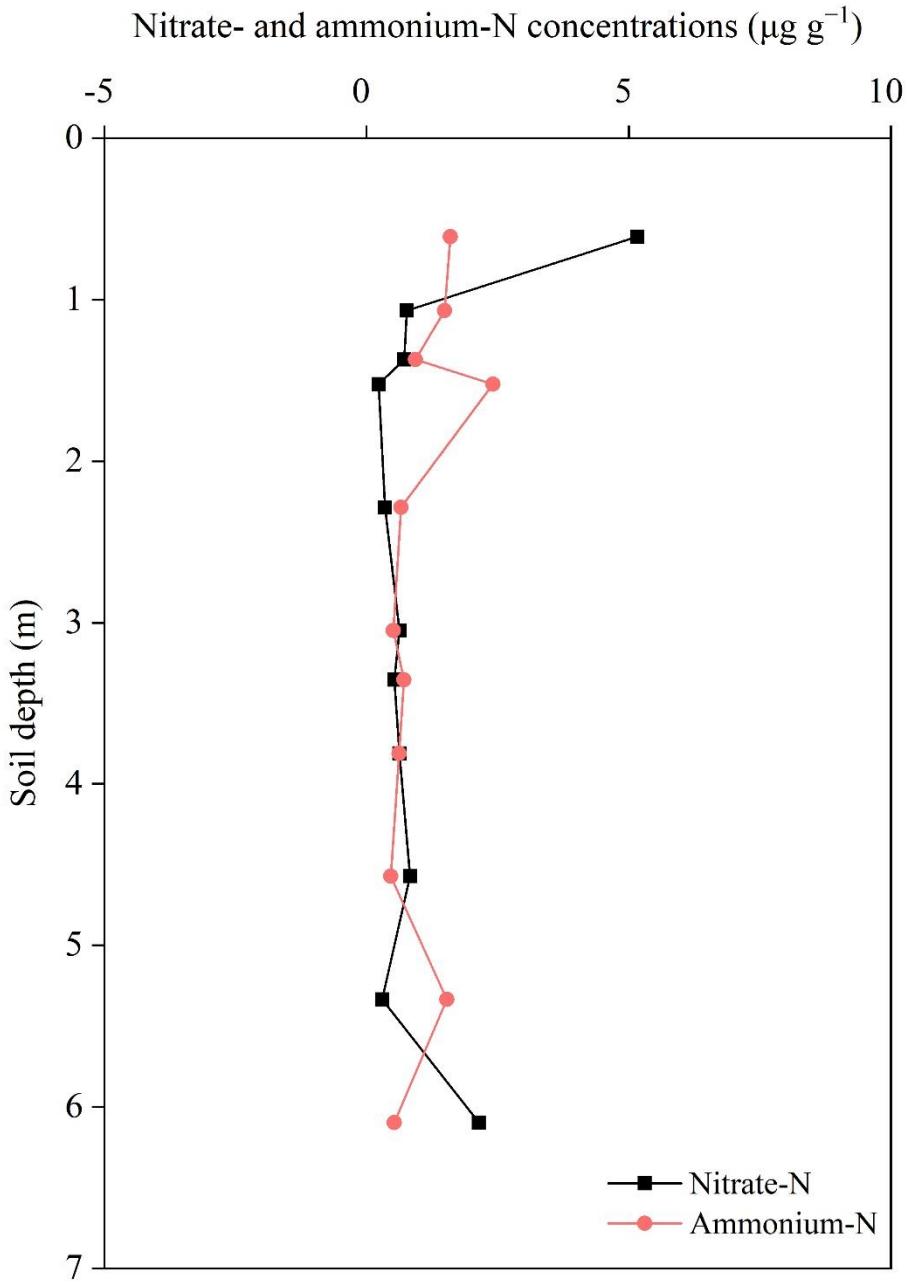

Fig. S24. Site MSEA3.

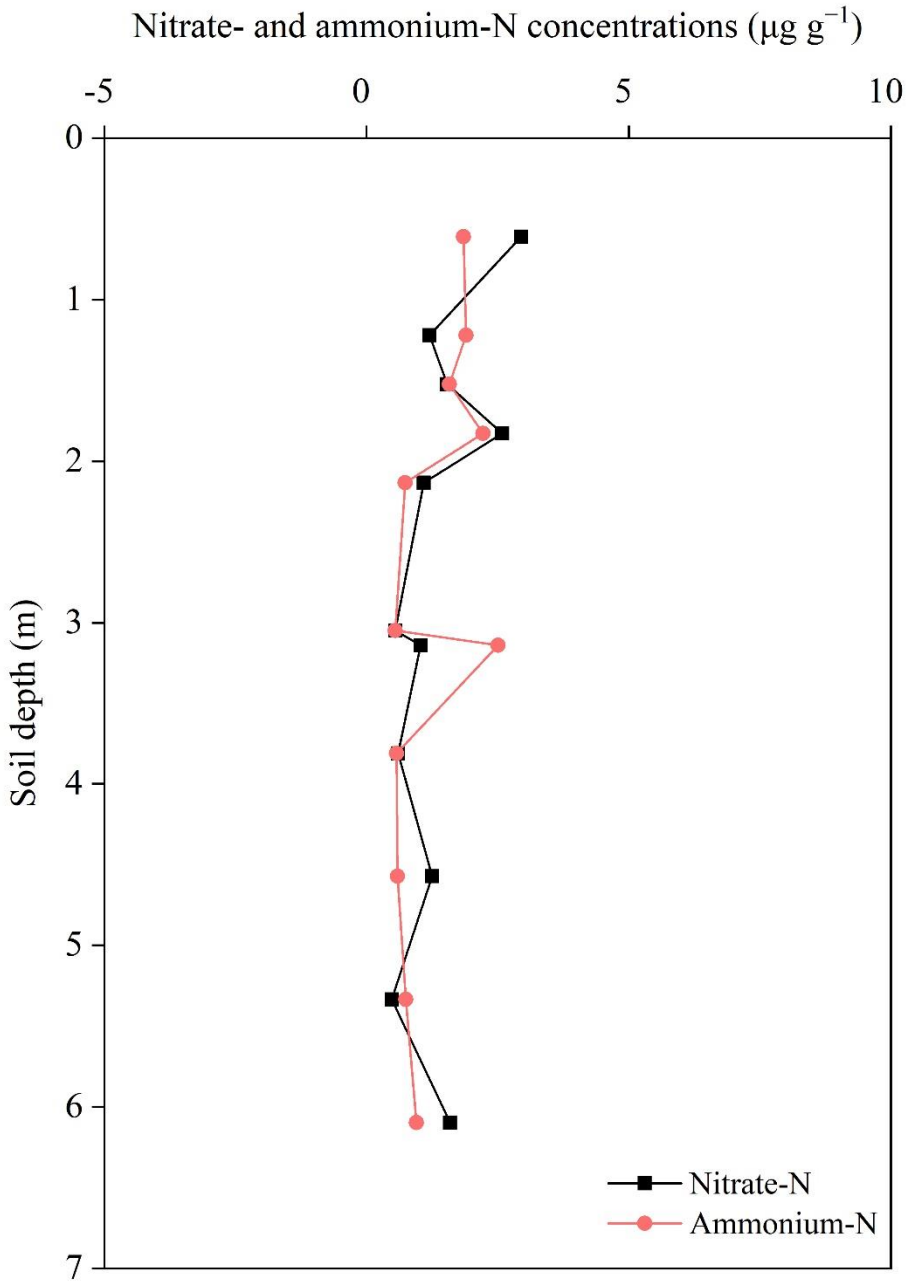

Fig. S25. Site MSEA6.

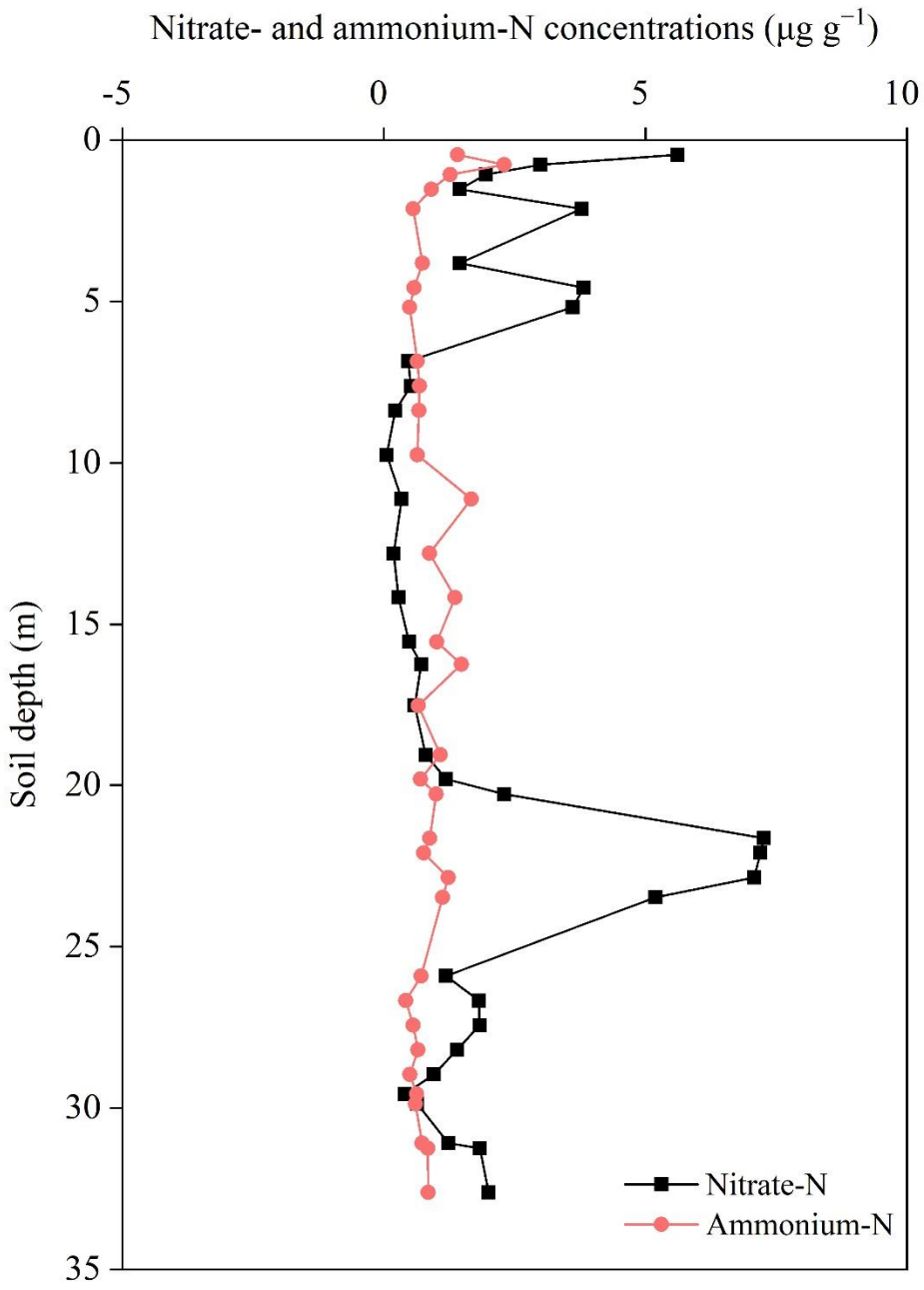

Fig. S26. Site Rosenau17.

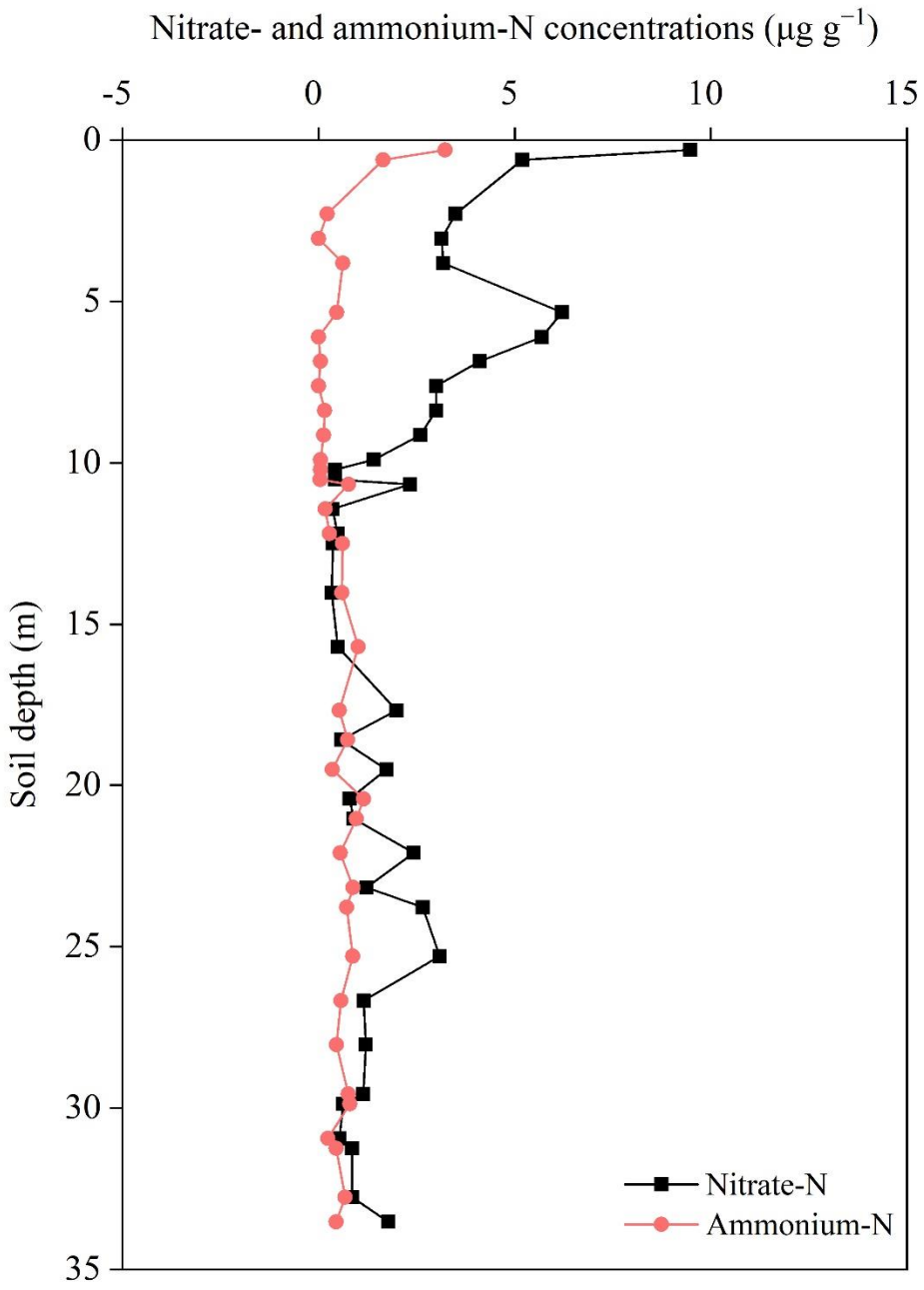

Fig. S27. Site RS1.

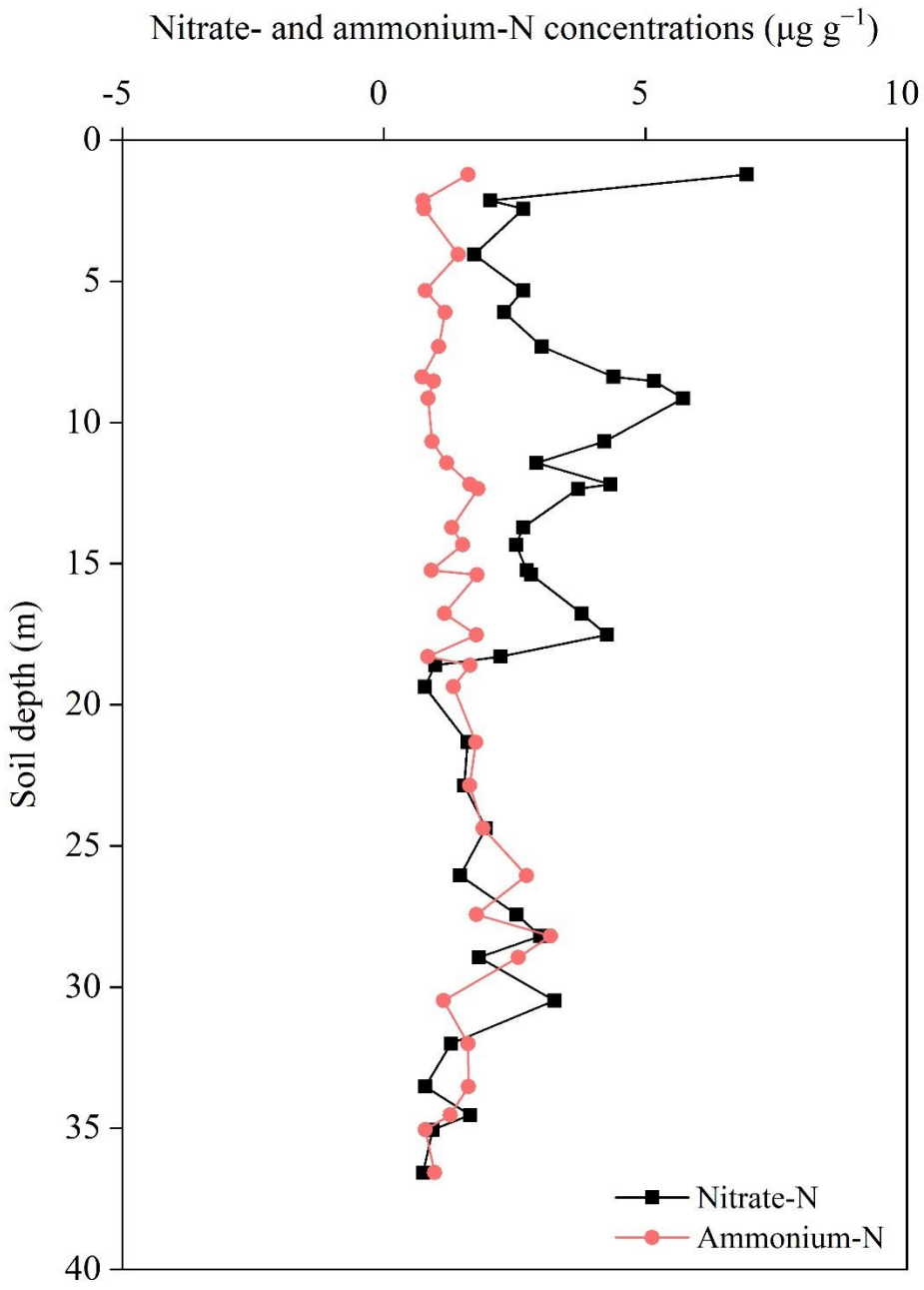

Fig. S28. Site RS6.

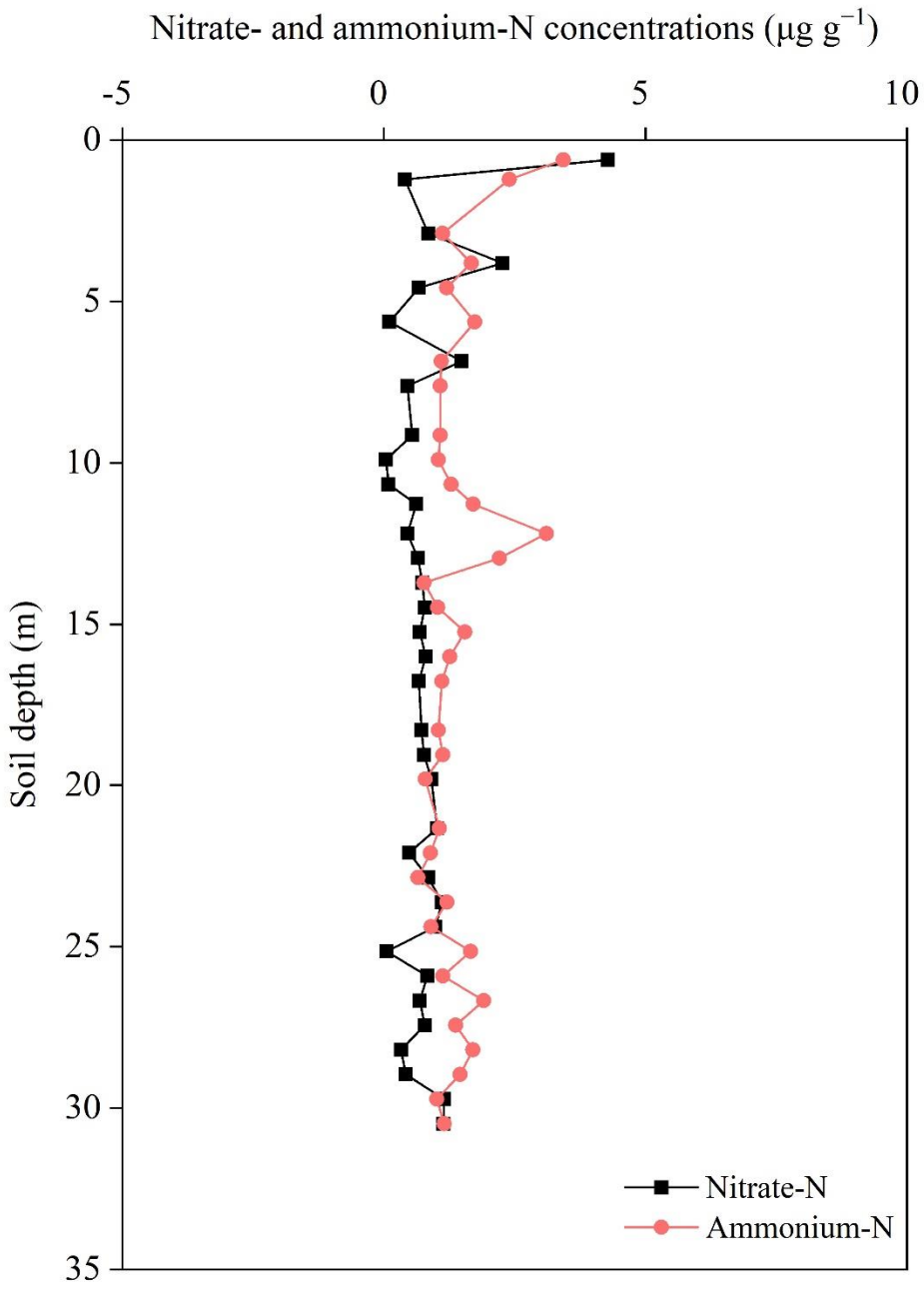

Fig. S29. Site RS8.

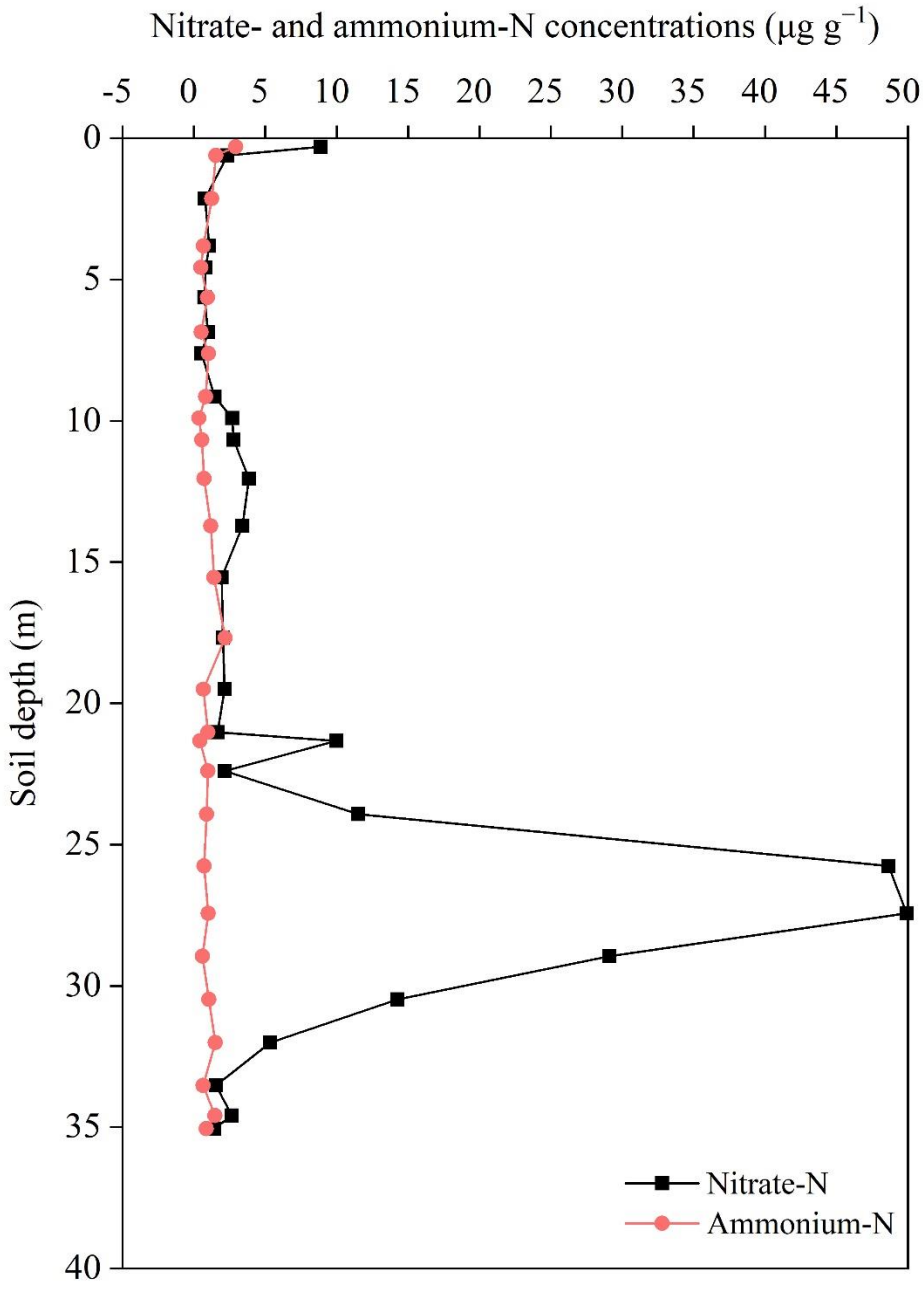

Fig. S30. Site RS9.

Table S1

Site ID, coordinates, sampling dates, and rig type used for coring

Site ID	Latitude	Longitude	Sampling Dates	Rig Type
DH-19	40.709581	-98.434800	3/29/16	CME
DH-20	40.774889	-98.285778	4/6/16	CME
DH-21	40.976983	-98.641439	11/16/16	CME
DH-22	41.188994	-97.737481	11/15/16	CME
DH-26	41.025300	-100.129444	12/11/19	CME
DH-28	40.749067	-100.01183	11/7/17	CME
DH-29	40.709528	-100.20247	11/6/17	CME
DH-30	40.773861	-99.397389	4/19/17	CME
DH-31	40.957383	-98.648400	11/21/16	CME
DH-32	40.738806	-98.360778	4/4/16	CME
DH-36	41.237247	-97.533028	11/15/16	CME
DH-37	40.822700	-99.491111	4/23/18	CME
DH-38	40.9883	-100.1438	4/23/18	CME
DH-39	41.016711	-100.2121	12/10/19	CME
DH-40	41.133700	-100.146389	4/23/18	CME
DH-41	41.169500	-99.799167	4/24/18	CME
DH-47	40.728472	-98.327528	3/30/16	CME
DH-48	40.698639	-98.316222	3/30/16	CME
DH-49	40.757639	-98.343361	3/31/16	CME
DH-50	40.7322	-99.9057	1/15/20	CME
MSEA-3	40.755617	-98.752772	11/14/17	GeoProbe
MSEA-6	40.753761	-98.755447	11/14/17	GeoProbe
Rosenau-17	40.732244	-99.905953	11/8/2017 & 12/12/19	CME
RS-1	41.0036	-99.6449	1/14/20	CME
RS-6	40.858389	-99.221806	4/18/17	CME
RS-8	40.896444	-98.815056	4/20/17	CME
RS-9	40.889333	-99.231222	4/19/17	CME

Table S2

Description of location ground water quality phase, irrigation method, and self-reported crop type and fertilizer application rates.

Site	GW Quality Phase	Irrigation Method	Crop Type (Self-Reported)	Fertilizer Application Rate (Self-Reported)
DH-19	Phase 2	Pivot	Corn/Seed Corn/Bean/Alfalfa rotation	1 ton of chicken manure - organic field for 8 years
DH-20	Phase 2	Pivot	Corn/Bean rotation	Average of 180 lbs/acre - field grid sampled every year, applied as recommended
DH-21	Phase 1	Pivot	Not Reported	Not Reported
DH-22	Phase 1	Pivot	Crop rotation	Actual N 230-240 lbs/acre every other year
DH-26	Phase 1	Pivot	Not Reported	Not Reported
DH-28	Phase 1	Gravity	Not Reported	Not Reported
DH-29	Phase 1	Gravity	Not Reported	Not Reported
DH-30	Phase 1	Pivot	Not Reported	Not Reported
DH-31	Phase 1	Pivot	Corn	Average 220 lbs/acre varies by nitrogen carryover from year to year using soil tests
DH-32	Phase 2	Pivot		
DH-36	Phase 1	Pivot	Corn/bean rotation	180-200 lbs-N/acre for corn
DH-37	Phase 1	Pivot	Not Reported	Not Reported
DH-38	Phase 1	Pivot	Not Reported	Not Reported
DH-39	Phase 1	Pivot	Not Reported	Not Reported
DH-40	Phase 1	Gravity	Not Reported	Not Reported
DH-41	Phase 1	Gravity	Not Reported	Not Reported
DH-47	Phase 1	Pivot	Corn/Seed Corn/Bean rotation	100 lbs-N/acre for seed corn and 220 lbs-N/acre for field corn
DH-48	Phase 1	Pivot	Corn/Seed Corn/Bean rotation	220 lbs-N/acre when continuos corn and 110 lbs-N/acre when corn/soybean rotation
DH-49	Phase 1	Gravity	Corn/Soybeans	Approximately 180 lbs-N/acre for corn
DH-50	Phase 1	Pivot	Not Reported	Not Reported
MSEA-3	Phase 3	Pivot	Not Reported	Not Reported
MSEA-6	Phase 3	Pivot	Not Reported	Not Reported
Rosenau-17	Phase 1	Pivot	Not Reported	Not Reported
RS-1	Phase 1	Pivot	Not Reported	Not Reported
RS-6	Phase 1	Pivot	Not Reported	Not Reported
RS-8	Phase 1	Pivot	Not Reported	Not Reported
RS-9	Phase 1	Pivot	Not Reported	Not Reported

Table S3

Sampling depth and depth of water table. “Refusal” indicates that the water table was not reached.

Site ID	Sampling Depth	Depth of water table
DH-19	28.47	28.47
DH-20	18.23	18.23
DH-21	36.52	36.50
DH-22	34.59	34.59
DH-26	24.23	24.23
DH-28	39.62	Refusal
DH-29	42.67	Refusal
DH-30	19.81	19.81
DH-31	33.22	33.22
DH-32	25.30	25.30
DH-36	37.95	37.95
DH-37	14.60	14.60
DH-38	21.34	21.34
DH-39	32.92	32.92
DH-40	24.38	Refusal
DH-41	33.68	33.68
DH-47	25.91	25.91
DH-48	22.86	22.86
DH-49	21.31	21.31
DH-50	45.42	Refusal
MSEA-3	6.10	6.10
MSEA-6	6.10	6.10
Rosenau-17	33.53	33.53
RS-1	32.92	32.92
RS-6	36.58	36.58
RS-8	30.48	30.48
RS-9	35.05	35.05

Table S4

Site ID	Vadose zone thickness (m)	Thickness category	Nitrate-N (g m^{-2})	Ammonium-N (g m^{-2})	Inorganic N (g m^{-2})	Nitrate-N (g m^{-2} m^{-1})	Ammonium-N (g m^{-2} $^{-1}$)
MSEA3	6	low	12.2	9.5	21.7	2.0	1.6
MSEA6	6	low	11.9	10.0	21.8	1.9	1.6
DH37	15	low	27.7	21.1	48.8	1.8	1.4
DH20	18	low	402.9	64.0	467.0	22.0	3.5
DH30	20	low	255.6	29.9	285.5	12.9	1.5
DH38	21	low	53.3	22.1	75.4	2.6	1.1
DH49	21	low	68.3	44.3	112.6	3.2	2.1
DH48	23	low	126.7	24.2	151.0	5.5	1.1
DH26	23	low	52.2	29.9	82.2	2.2	1.3
DH40	24	high	142.7	31.7	174.5	6.0	1.3
DH32	26	high	25.2	40.4	65.6	1.0	1.6
DH47	26	high	61.0	11.5	72.5	2.4	0.4
DH19	29	high	1010.4	33.3	1043.6	35.3	1.2
RS8	30	high	36.8	61.1	97.9	1.2	2.0
Rosenau17	33	high	78.5	41.4	120.0	2.4	1.3
DH31	34	high	258.8	22.3	281.1	7.7	0.7
DH39	34	high	146.4	43.8	190.2	4.4	1.3
RS1	34	high	87.9	24.1	112.0	2.6	0.7
DH22	34	high	103.1	64.6	167.7	3.0	1.9
DH41	34	high	74.4	45.7	120.1	2.2	1.3
RS9	35	high	452.9	49.1	502.1	12.9	1.4
DH21	37	high	237.7	112.3	350.0	6.5	3.1
RS6	37	high	148.2	88.3	236.5	4.1	2.4
DH36	37	high	146.2	37.6	183.8	3.9	1.0
DH28	39	high	262.8	49.8	312.6	6.8	1.3
DH29	42	high	443.6	76.6	520.2	10.6	1.8
DH50	45	high	137.3	80.9	218.2	3.1	1.8